Studying Neutron Star interior

using unified relativistic mean-field equations of state

Luigi Scurto, Helena Pais, Francesca Gulminelli

QNP Symposium 2024

How compact?

Neutron Star	Sun
$M \approx 1.4 - 2.0 M_\odot$	$M = 1 M_\odot$
$R \approx 11 - 14 km$	$R \approx 700.000 km$

$$\rho_{NS} \approx 1.000.000.000.000 \rho_\odot$$

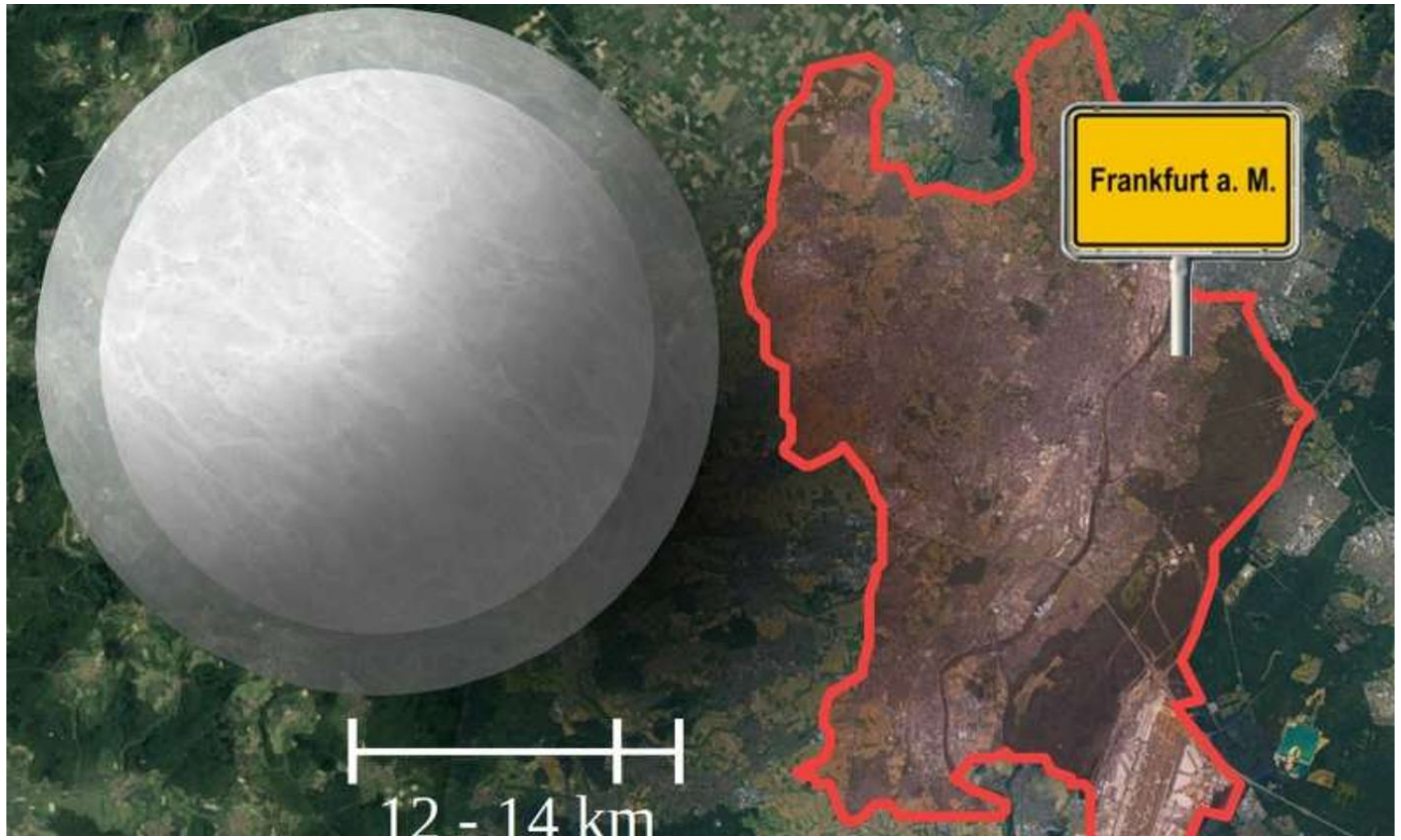

Credit: Lukas Weih, Goethe University

Roughly a trillion times denser than the sun !

How to probe the interior structure

Einstein Theory of General Relativity connects the interior composition of the NS to the mass and radius via the Tolman–Oppenheimer–Volkoff equations

$$
\begin{aligned}
\frac{dP}{dr} &= -\frac{Gm\varepsilon}{c^2r^2}\left(1+\frac{P}{\varepsilon}\right)\left(1+\frac{4\pi r^3 P}{mc^2}\right)\left(1-\frac{2Gm}{c^2r}\right)^{-1} \\
\frac{dm}{dr} &= 4\pi\frac{\varepsilon}{c^2}r^2 \,.
\end{aligned}
$$

How to probe the interior structure

Einstein Theory of General Relativity connects the interior composition of the NS to the mass and radius via the Tolman–Oppenheimer–Volkoff equations

$$\frac{dP}{dr} = -\frac{Gm\varepsilon}{c^2r^2}\left(1+\frac{P}{\varepsilon}\right)\left(1+\frac{4\pi r^3 P}{mc^2}\right)\left(1-\frac{2Gm}{c^2 r}\right)^{-1}$$

$$\frac{dm}{dr} = 4\pi\frac{\varepsilon}{c^2}r^2 \,.$$

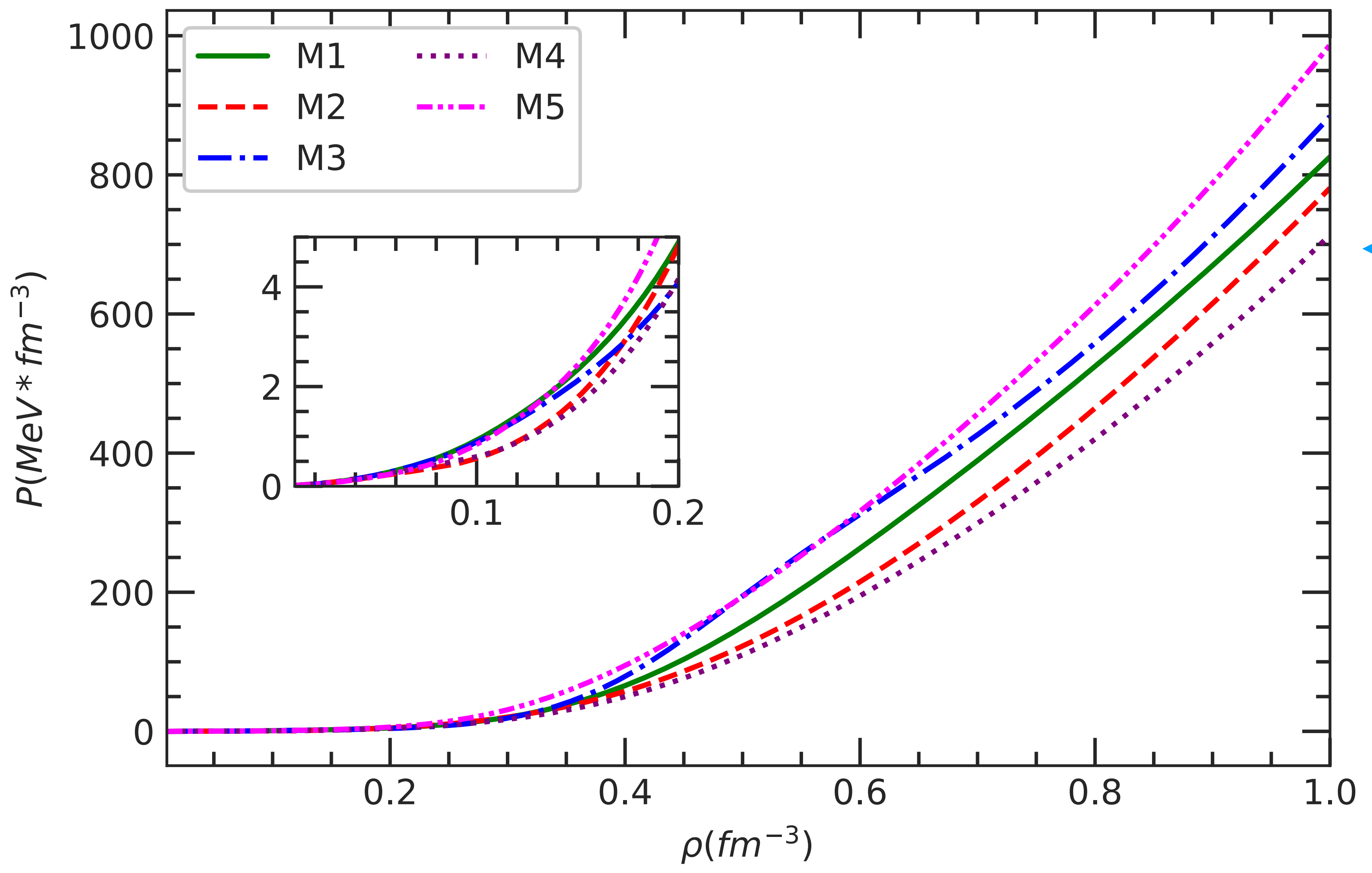

Connection between

Equation of State

and

Mass-Radius

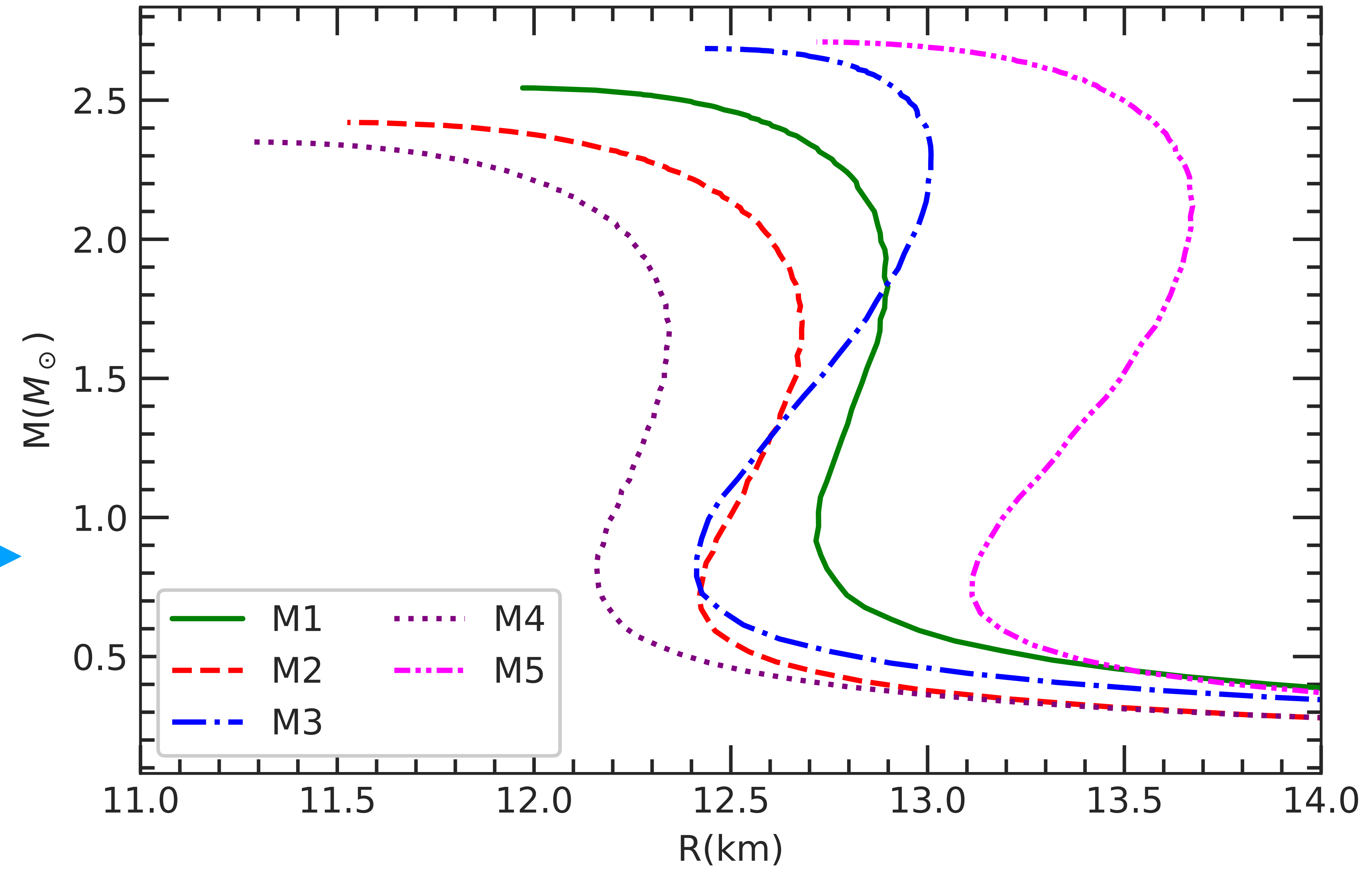

Framework

Relativistic Mean Field Approximation

In our work we use two different Relativistic Mean Field (RMF) models in order to describe stellar matter (npem). In this approximation, the interaction between nucleons is mediated by mesons.

$$\mathscr{L} = \sum_{i=p,n} \mathscr{L}_i + \mathscr{L}_l + \mathscr{L}_\sigma + \mathscr{L}_\omega + \mathscr{L}_\rho$$

Relativistic Mean Field Approximation

In our work we use two different Relativistic Mean Field (RMF) models in order to describe stellar matter (npem). In this approximation, the interaction between nucleons is mediated by mesons.

$$\mathscr{L} = \boxed{\sum_{i=p,n} \mathscr{L}_i} + \mathscr{L}_l + \mathscr{L}_\sigma + \mathscr{L}_\omega + \mathscr{L}_\rho$$

Nucleons

$$\mathscr{L}_i = \bar{\psi}_i \left[\gamma_\mu i \partial^\mu - g_\omega V^\mu - \frac{g_\rho}{2} \tau \cdot \mathbf{b}^\mu - M^* \right] \psi_i$$

$$M^* = M - g_\sigma \phi$$

Relativistic Mean Field Approximation

In our work we use two different Relativistic Mean Field (RMF) models in order to describe stellar matter (npem). In this approximation, the interaction between nucleons is mediated by mesons.

$$\mathscr{L} = \underbrace{\boxed{\sum_{i=p,n} \mathscr{L}_i}}_{\text{Nucleons}} + \underbrace{\boxed{\mathscr{L}_l}}_{\text{Leptons}} + \mathscr{L}_\sigma + \mathscr{L}_\omega + \mathscr{L}_\rho$$

Leptons

$$\mathscr{L}_l = \sum_{i=e,\mu} \bar{\psi}_i [\gamma_\mu i\partial^\mu - m_i] \psi_i$$

Nucleons

$$\mathscr{L}_i = \bar{\psi}_i \left[\gamma_\mu i\partial^\mu - g_\omega V^\mu - \frac{g_\rho}{2} \tau \cdot \mathbf{b}^\mu - M^* \right] \psi_i$$

$$M^* = M - g_\sigma \phi$$

Relativistic Mean Field Approximation

In our work we use two different Relativistic Mean Field (RMF) models in order to describe stellar matter (npem). In this approximation, the interaction between nucleons is mediated by mesons.

$$\mathscr{L} = \boxed{\sum_{i=p,n} \mathscr{L}_i} + \boxed{\mathscr{L}_l} + \boxed{\mathscr{L}_\sigma + \mathscr{L}_\omega + \mathscr{L}_\rho}$$

Nucleons

Leptons

$$\mathscr{L}_l = \sum_{i=e,\mu} \bar{\psi}_i \left[\gamma_\mu i\partial^\mu - m_i\right]\psi_i$$

Mesons

$$\mathscr{L}_\sigma = \frac{1}{2}\left(\partial_\mu\phi\partial^\mu\phi - m_\sigma^2\phi^2\right)$$

$$\mathscr{L}_\rho = -\frac{1}{4}\mathbf{B}_{\mu\nu}\cdot\mathbf{B}^{\mu\nu} + \frac{1}{2}m_\rho^2\mathbf{b}_\mu\cdot\mathbf{b}^\mu$$

$$\mathscr{L}_\omega = -\frac{1}{4}\Omega_{\mu\nu}\Omega^{\mu\nu} + \frac{1}{2}m_\omega^2 V_\mu V^\mu$$

The mesons are then replaced with their ground state expectation value

$$\mathscr{L}_i = \bar{\psi}_i\left[\gamma_\mu i\partial^\mu - g_\omega V^\mu - \frac{g_\rho}{2}\tau\cdot\mathbf{b}^\mu - M^*\right]\psi_i$$

$$M^* = M - g_\sigma\phi$$

Relativistic Mean Field Approximation

In our work we use two different Relativistic Mean Field (RMF) models in order to describe stellar matter (npem). In this approximation, the interaction between nucleons is mediated by mesons.

$$\mathscr{L} = \sum_{i=p,n} \mathscr{L}_i + \mathscr{L}_l + \mathscr{L}_\sigma + \mathscr{L}_\omega + \mathscr{L}_\rho$$

Nucleons

Leptons

$$\mathscr{L}_l = \sum_{i=e,\mu} \bar{\psi}_i [\gamma_\mu i\partial^\mu - m_i] \psi_i$$

Mesons

$$\mathscr{L}_\sigma = \frac{1}{2}\left(\partial_\mu \phi \partial^\mu \phi - m_\sigma^2 \phi^2\right)$$

$$\mathscr{L}_\rho = -\frac{1}{4}\mathbf{B}_{\mu\nu} \cdot \mathbf{B}^{\mu\nu} + \frac{1}{2} m_\rho^2 \mathbf{b}_\mu \cdot \mathbf{b}^\mu$$

$$\mathscr{L}_\omega = -\frac{1}{4}\Omega_{\mu\nu}\Omega^{\mu\nu} + \frac{1}{2} m_\omega^2 V_\mu V^\mu$$

The mesons are then replaced with their ground state expectation value

$$\mathscr{L}_i = \bar{\psi}_i \left[\gamma_\mu i\partial^\mu - g_\omega V^\mu - \frac{g_\rho}{2} \tau \cdot \mathbf{b}^\mu - M^*\right] \psi_i$$

$$M^* = M - g_\sigma \phi$$

Nucleon-Meson couplings

Nucleon-Meson Couplings

In our study we consider the couplings being a function of the baryonic density

$$g_i = a_i + (b_i + d_i x^3)e^{-c_i x} \qquad \text{with} \qquad x = \rho/\rho_0$$

P. Gogelein, E.N.E. van Dalen, C. Fuchs and H. Muther, Phys. Rev. C 77, 025802 (2008)

Nucleon-Meson Couplings

In our study we consider the couplings being a function of the baryonic density

$$g_i = a_i + (b_i + d_i x^3) e^{-c_i x} \quad \text{with} \quad x = \rho / \rho_0$$

Saturation density of the model

P. Gogelein, E.N.E. van Dalen, C. Fuchs and H. Muther, Phys. Rev. C 77, 025802 (2008)

Nucleon-Meson Couplings

In our study we consider the couplings being a function of the baryonic density

$$g_i = a_i + (b_i + d_i x^3) e^{-c_i x} \quad \text{with} \quad x = \rho/\rho_0$$

Saturation density of the model

P. Gogelein, E.N.E. van Dalen, C. Fuchs and H. Muther, Phys. Rev. C 77, 025802 (2008)

Each model is uniquely defined by a set 12 parameters (4 per coupling)

Nucleon-Meson Couplings

In our study we consider the couplings being a function of the baryonic density

$$g_i = a_i + (b_i + d_i x^3) e^{-c_i x} \quad \text{with} \quad x = \rho / \rho_0$$

Saturation density of the model

P. Gogelein, E.N.E. van Dalen, C. Fuchs and H. Muther, Phys. Rev. C 77, 025802 (2008)

Each model is uniquely defined by a set 12 parameters (4 per coupling)

The same set of parameters is used for crust and core

Neutron Star Crust

For the description of the crust, we use a Compressible Liquid Drop approximation and a Wiegner-Seitz (WS) cell approximation to describe our system

Neutron Star Crust

For the description of the crust, we use a Compressible Liquid Drop approximation and a Wiegner-Seitz (WS) cell approximation to describe our system

- **Matter is divided into cells**

Neutron Star Crust

For the description of the crust, we use a Compressible Liquid Drop approximation and a Wiegner-Seitz (WS) cell approximation to describe our system

- **Matter is divided into cells**
- **Matter in each cell is divided into a denser (liquid) phase and a less dense (gas) phase**

Neutron Star Crust

For the description of the crust, we use a Compressible Liquid Drop approximation and a Wiegner-Seitz (WS) cell approximation to describe our system

- **Matter is divided into cells**
- **Matter in each cell is divided into a denser (liquid) phase and a less dense (gas) phase**
- **The total energy density of the system is given by**

$$\mathcal{E} = f\mathcal{E}^{I} + (1-f)\mathcal{E}^{II} + \mathcal{E}_{Coul} + \mathcal{E}_{surf} + \mathcal{E}_{e} .$$

Where

$f =$ fraction of liquid phase

$\mathcal{E}^{i} =$ energy density of phase I

$\mathcal{E}_{e} =$ energy density of electrons

$$\mathcal{E}_{Coul} = 2\alpha e^2 \pi \Phi R_d^2 \left(\rho_p^I - \rho_p^{II}\right)^2$$

$$\mathcal{E}_{surf} = \frac{\sigma\alpha D}{R_d}$$

Neutron Star Crust

For the description of the crust, we use a Compressible Liquid Drop approximation and a Wiegner-Seitz (WS) cell approximation to describe our system

- **Matter is divided into cells**
- **Matter in each cell is divided into a denser (liquid) phase and a less dense (gas) phase**
- **The total energy density of the system is given by**

$$\mathscr{E} = f\mathscr{E}^I + (1-f)\mathscr{E}^{II} + \mathscr{E}_{Coul} + \mathscr{E}_{surf} + \mathscr{E}_e\,.$$

Where

$f =$ **fraction of liquid phase**

$\mathscr{E}^i =$ **energy density of phase I**

$\mathscr{E}_e =$ **energy density of electrons**

$$\mathscr{E}_{Coul} = 2\alpha e^2 \pi \Phi R_d^2 \left(\rho_p^I - \rho_p^{II}\right)^2$$

$$\mathscr{E}_{surf} = \frac{\sigma\alpha D}{R_d}$$

Surface tension parameter

Surface tension parameter

For the surface tension parameter depends on the EoS. In order to calculate it we use the following expression

$$\sigma = \sigma_0 \frac{b + 2^4}{b + y_{p,I}^{-3} + (1 - y_{p,I})^{-3}}$$

Surface tension parameter

For the surface tension parameter depends on the EoS. In order to calculate it we use the following expression

$$\sigma = \sigma_0 \frac{b + 2^4}{b + y_{p,I}^{-3} + (1 - y_{p,I})^{-3}}$$

Proton fraction of liquid phase

Surface tension parameter

For the surface tension parameter depends on the EoS. In order to calculate it we use the following expression

$$\sigma = \sigma_0 \frac{b + 2^4}{b + y_{p,l}^{-3} + (1 - y_{p,l})^{-3}}$$

Proton fraction of liquid phase

This parameters are obtained via a fit over nuclear masses

We use the AME2016 nuclear masses table

M. Wang et al., Chinese Physics C41, 030003 (2017)

Already done in T. Carreau, F. Gulminelli and J. Margueron, Eur. Phys. J. A55, 188 (2019)

Astrophysical constraints

Astrophysical constraints

Maximum Mass

↓

PSR J0348+0432 mass has been measured very precisely to be

$$2.01 \pm 0.04 M_{\odot}$$

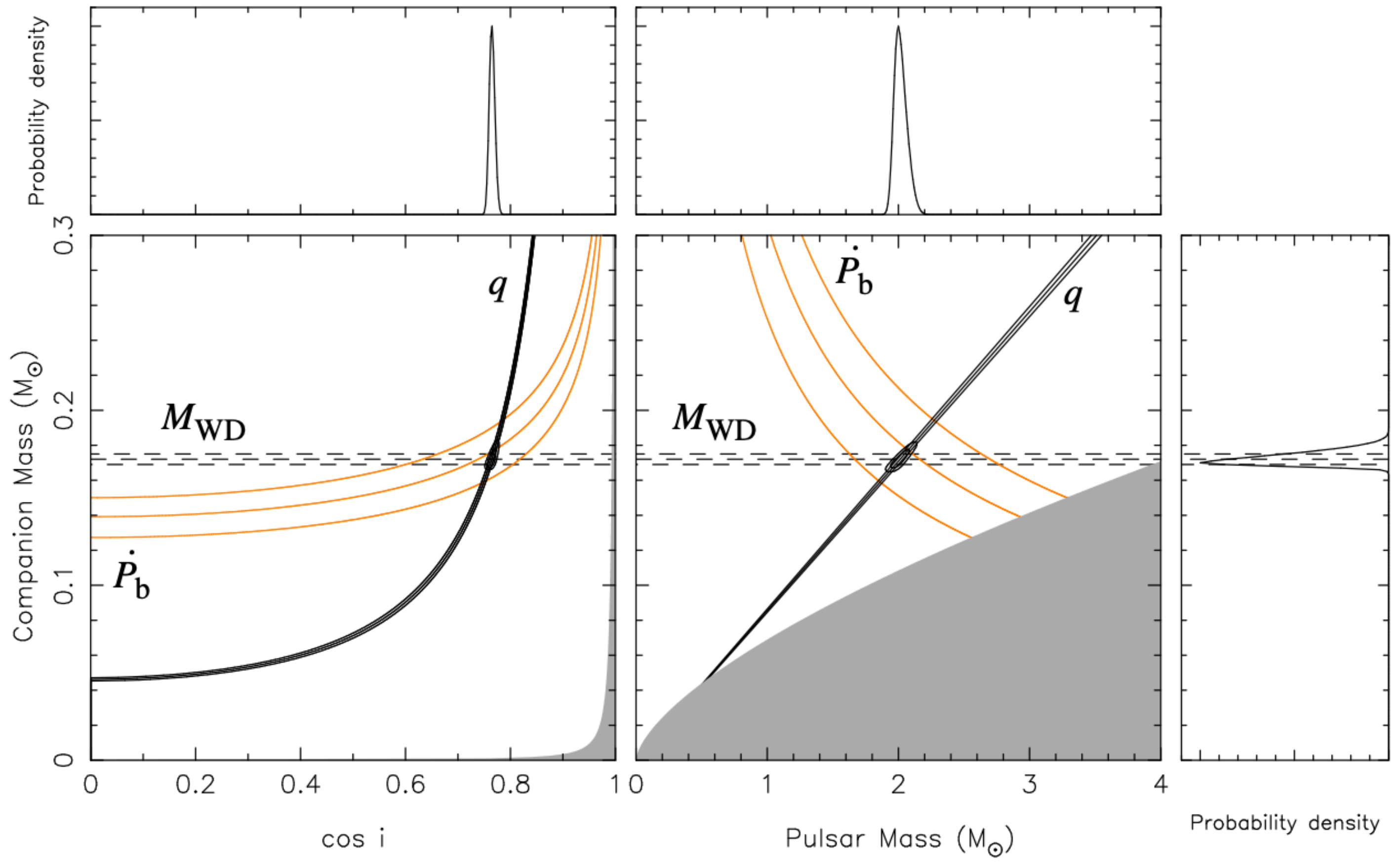

J. Antoniadis et al., Science 340, 6131 (2013)

Astrophysical constraints

Maximum Mass

PSR J0348+0432 mass has been measured very precisely to be

$$2.01 \pm 0.04 M_\odot$$

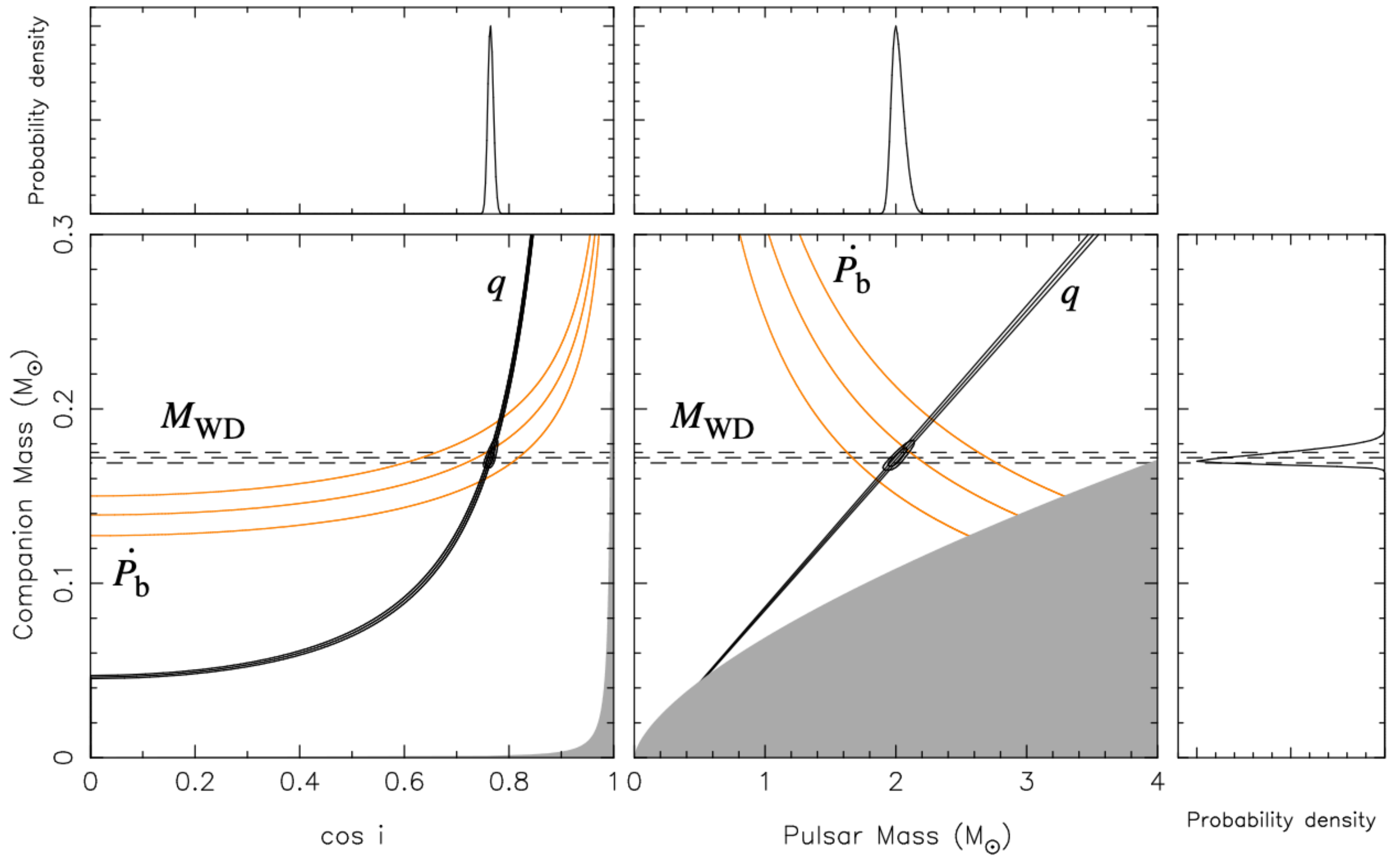

J. Antoniadis et al., Science 340, 6131 (2013)

GW170817

Gravitational signal coming from NS-NS merger

Constraint on the tidal deformability

$$\tilde{\Lambda} = \frac{16}{13}\frac{(m_1 + 12m_2)m_1^4\Lambda_1 + (m_2 + 12m_1)m_2^4\Lambda_2}{(m_1 + m_2)^5}$$

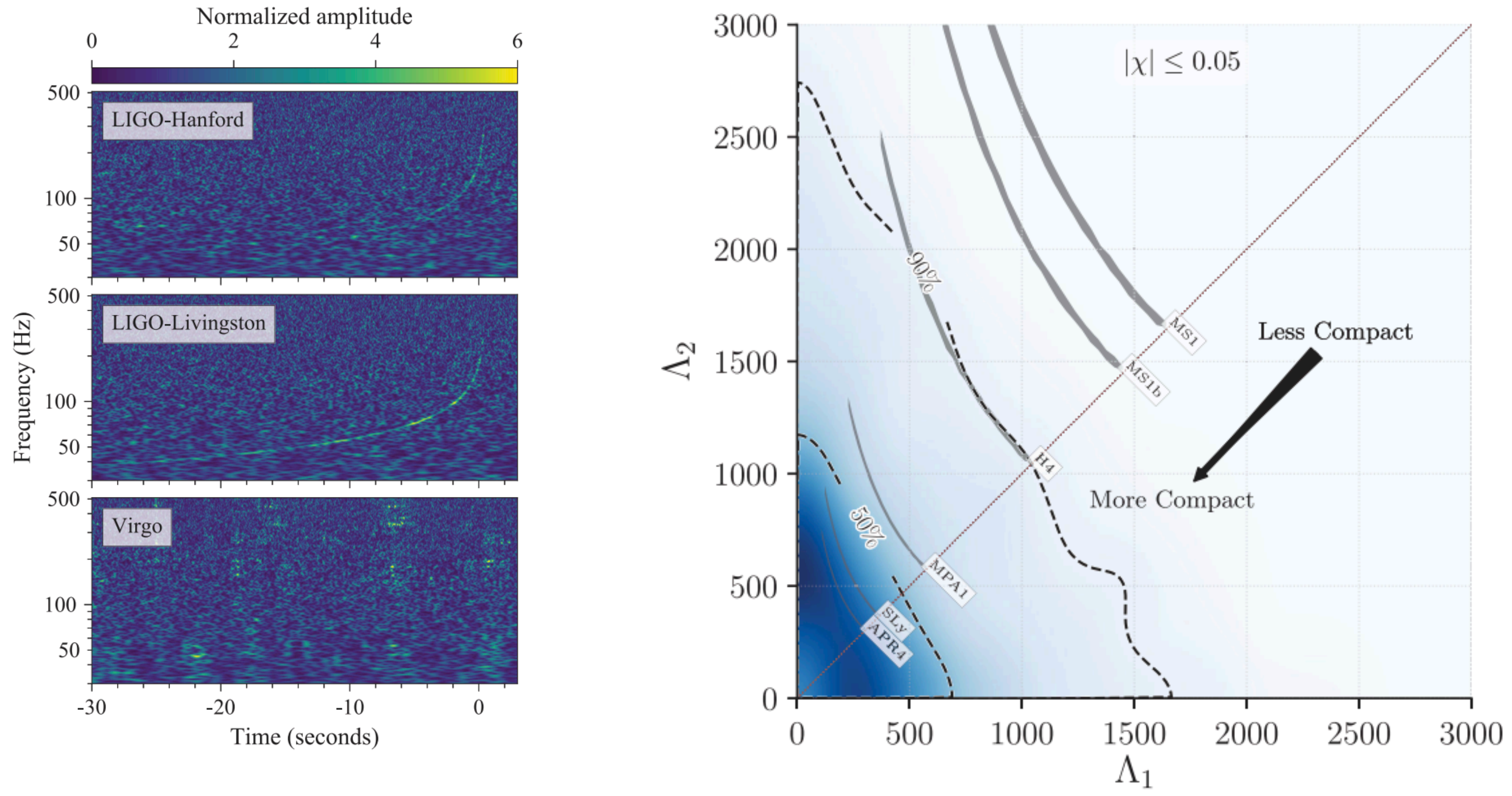

P.B. Abbott et al. (LIGO Scientific, Virgo), Phys. Rev. Lett. 121, 161101 (2017)

Astrophysical constraints

Maximum Mass

PSR J0348+0432 mass has been measured very precisely to be

$$2.01 \pm 0.04 M_\odot$$

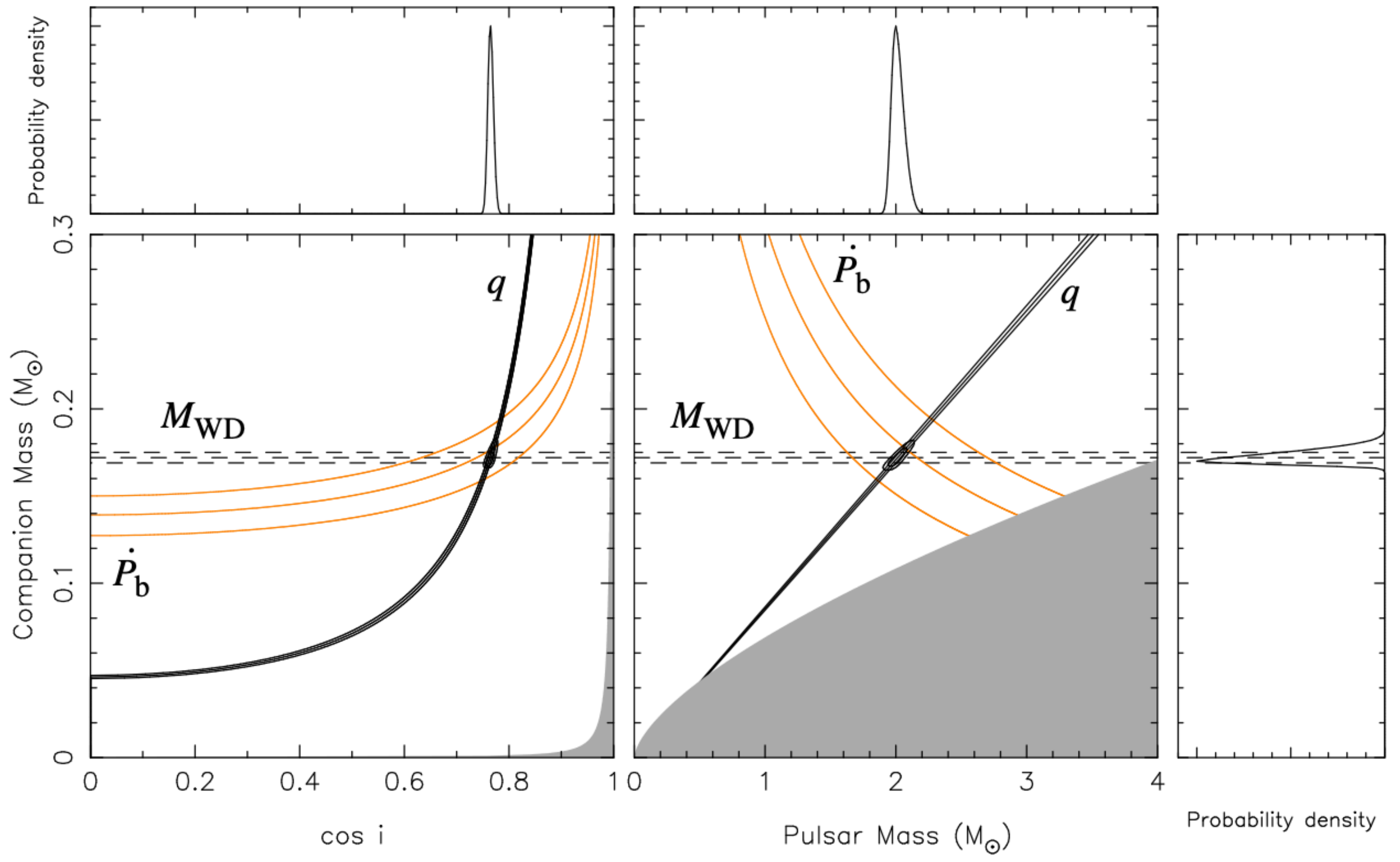

J. Antoniadis et al., Science 340, 6131 (2013)

GW170817

Gravitational signal coming from NS-NS merger

Constraint on the tidal deformability

$$\tilde{\Lambda} = \frac{16}{13}\frac{(m_1 + 12m_2)m_1^4\Lambda_1 + (m_2 + 12m_1)m_2^4\Lambda_2}{(m_1 + m_2)^5}$$

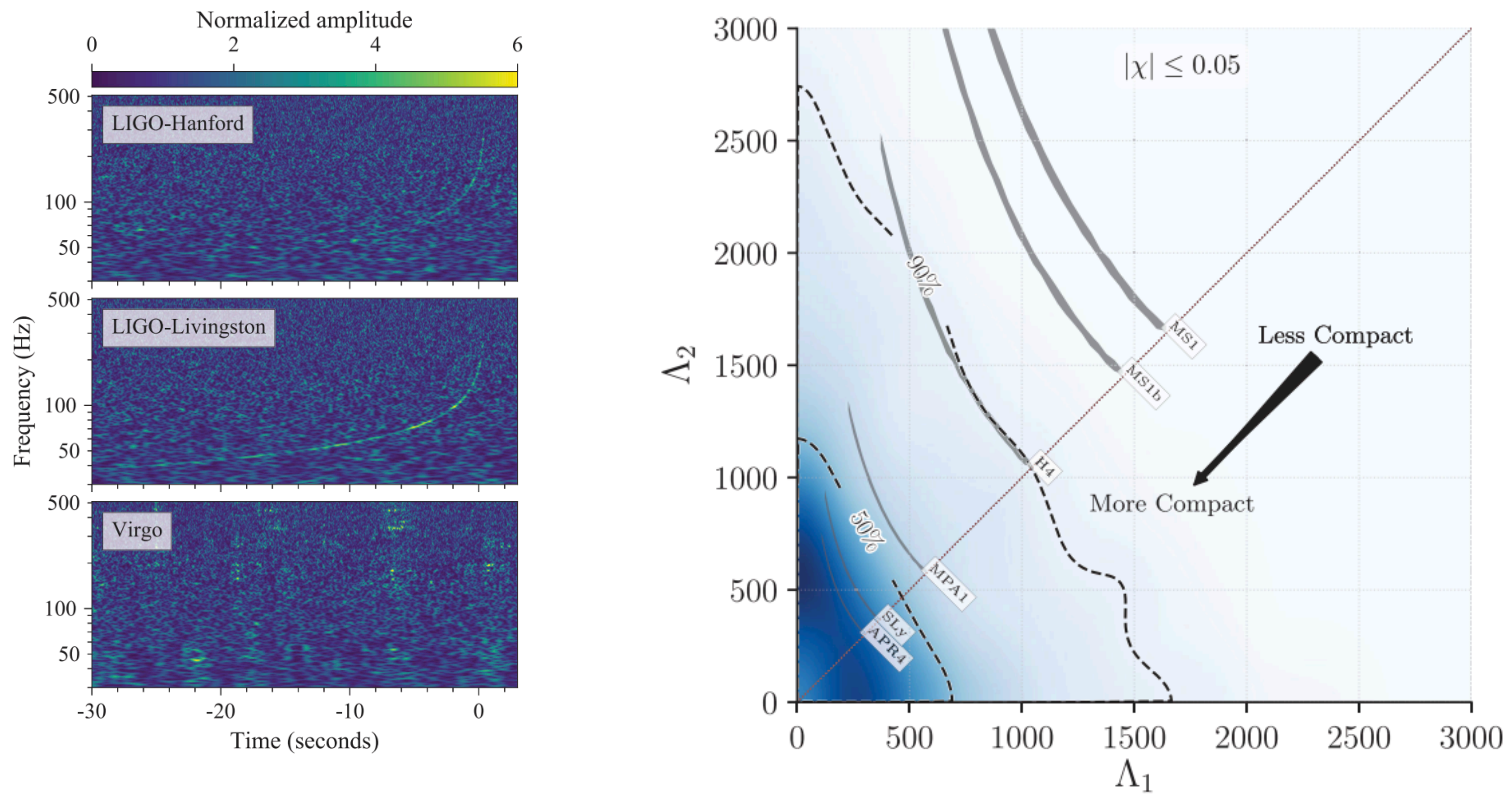

P.B. Abbott et al. (LIGO Scientific, Virgo), Phys. Rev. Lett. 121, 161101 (2017)

NICER

Measure of NS radius using hotspot tracking

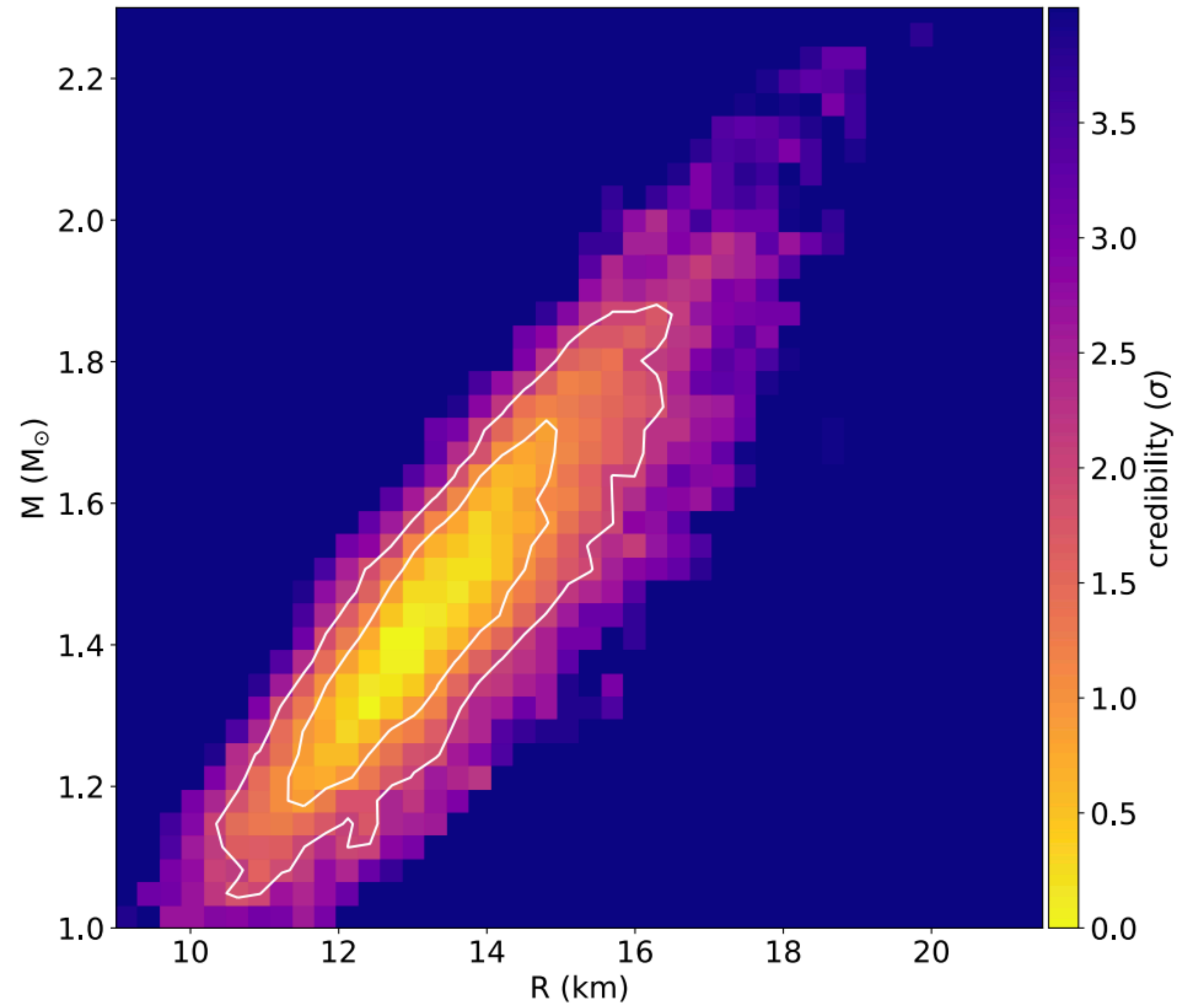

M.C. Miller et al., ApJL 887, L24 (2019)

M.C. Miller et al., ApjL 918, L28 (2021)

Nuclear constraints

Nuclear constraints

Theoretical Constraint

Chiral EFT constraints the EoS of neutron matter

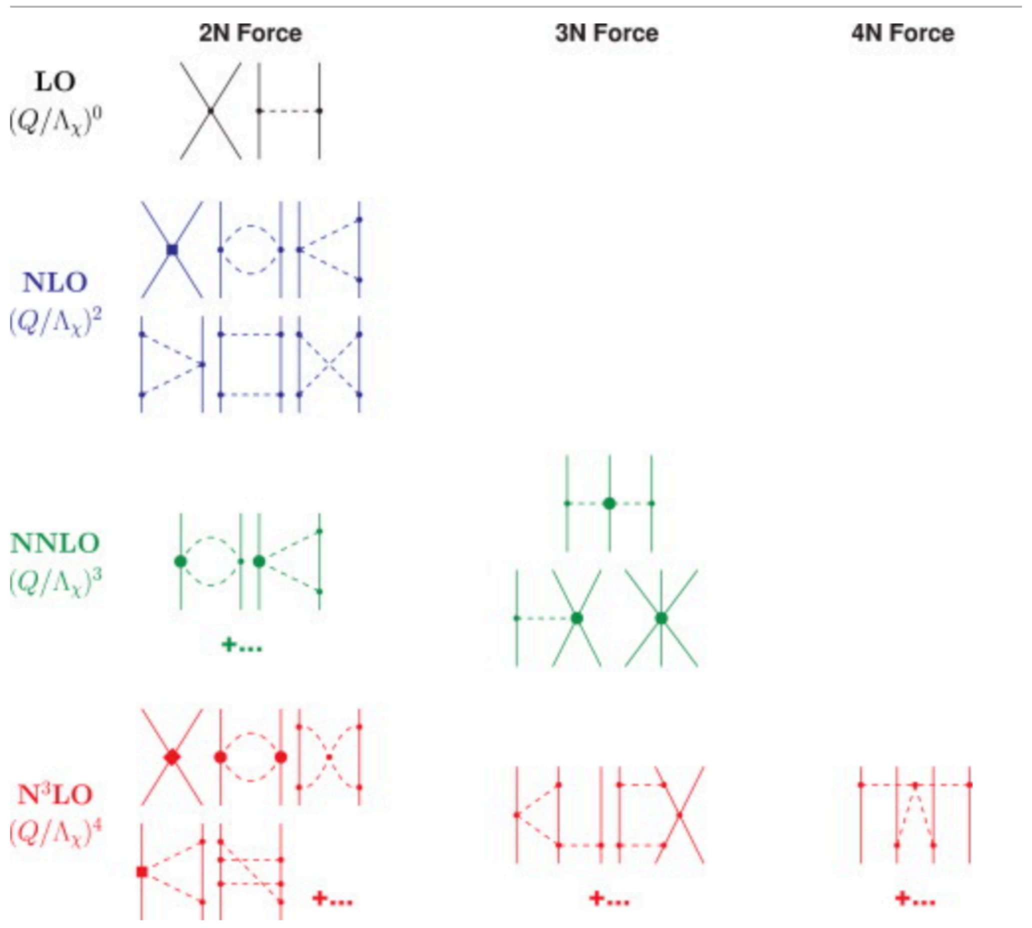

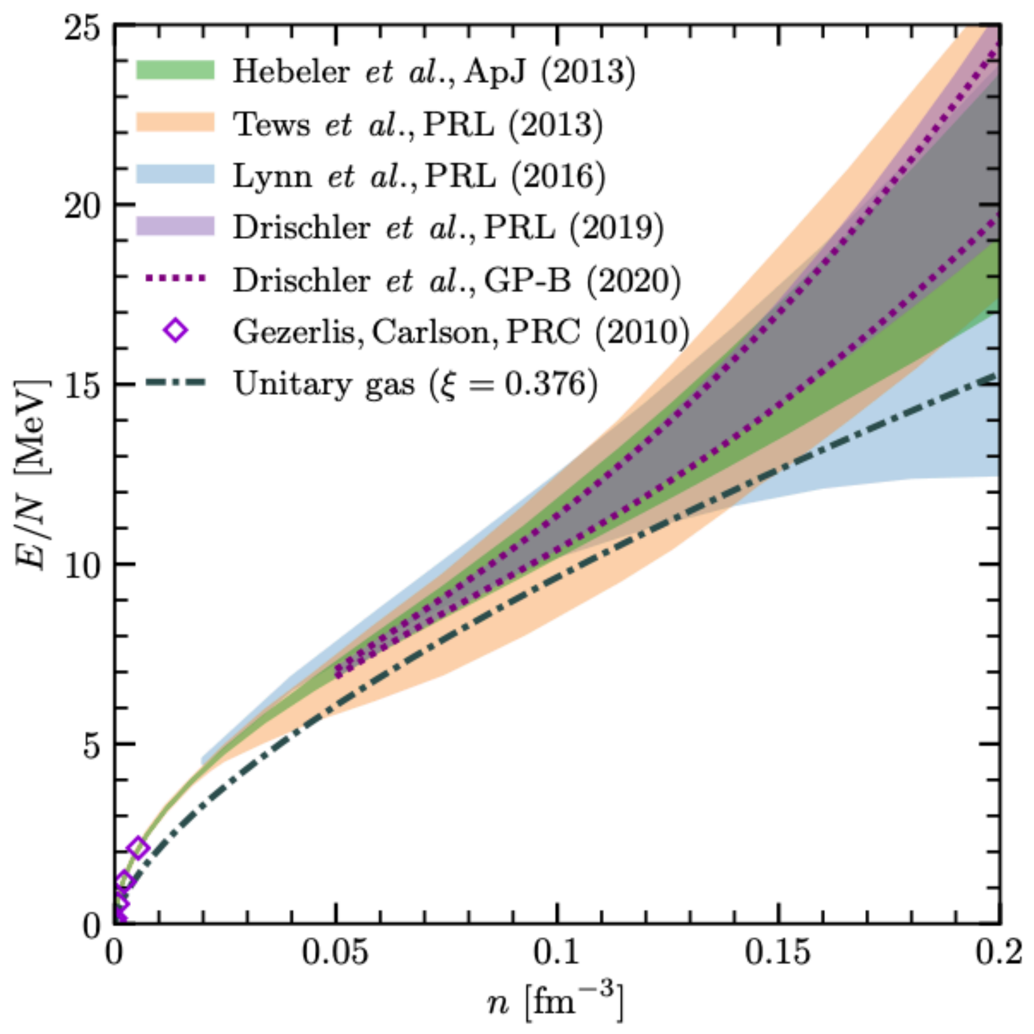

R. Machleidt, D.R. Entem, Physics Reports, 503, Issue 1, (2011)

S. Huth, C. Wellenhofer, A. Schwenk, Phys.Rev.C 103, 025803 (2021)

Nuclear constraints

Theoretical Constraint

Chiral EFT constraints the EoS of neutron matter

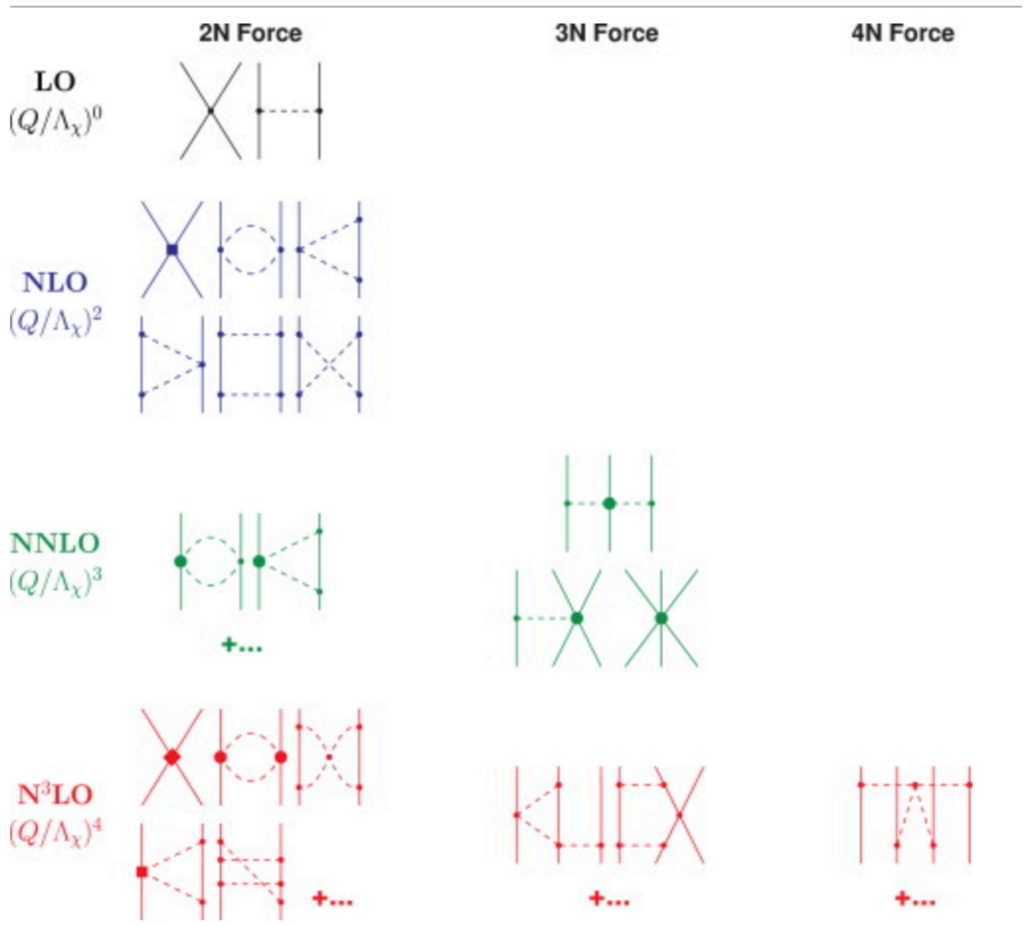

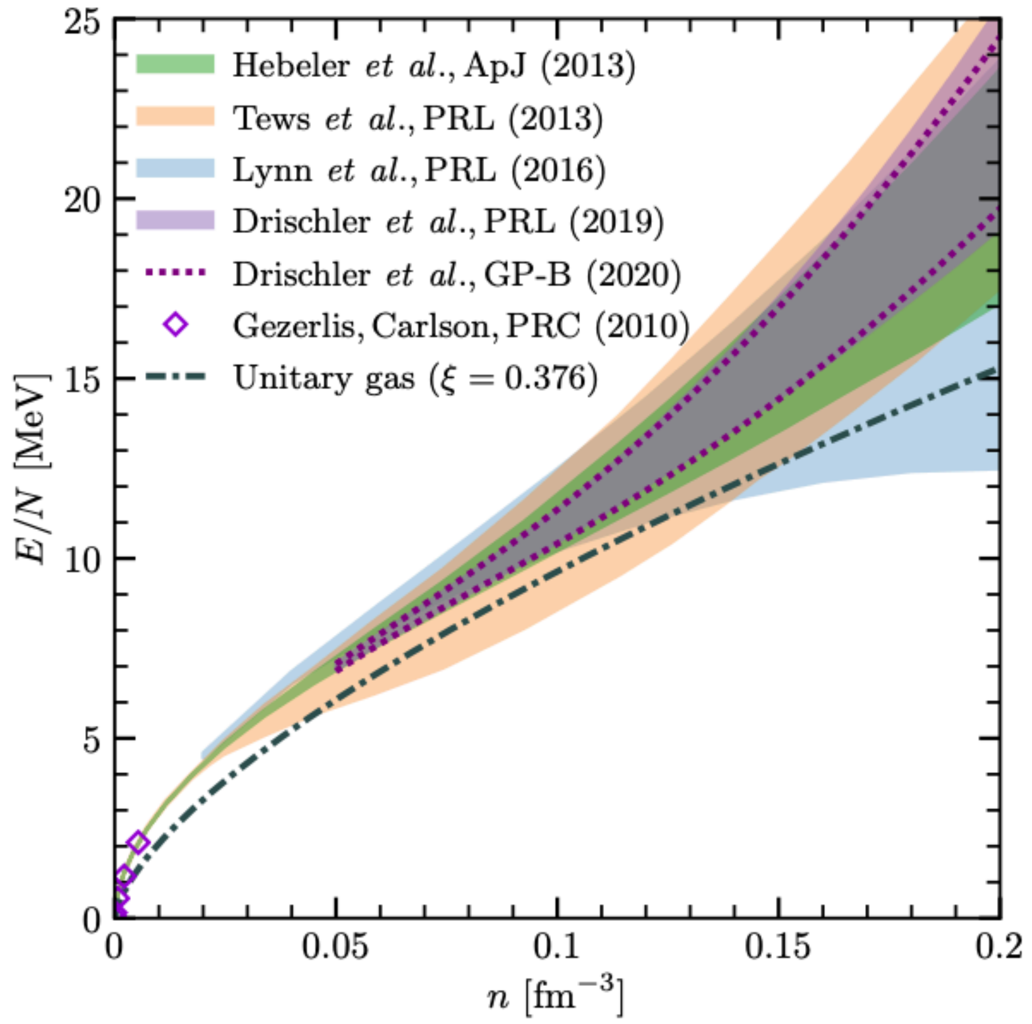

R. Machleidt, D.R. Entem, Physics Reports, 503, Issue 1, (2011)

S. Huth, C. Wellenhofer, A. Schwenk, Phys.Rev.C 103, 025803 (2021)

Experimental Constraint

Nuclear experiments constraint the derivatives of the energy per baryon of symmetric matter at saturation

	μ	σ
$\rho_{sat}(\mathrm{fm}^{-3})$	0.153	0.005
$E_{sat}(MeV)$	-15.8	0.3
$K_{sat}(MeV)$	230	20
$J_{sym}(MeV)$	32.0	2.0
$K_\tau(MeV)$	-400	100

$$K_\tau = K_{sym} - 6L_{sym} - Q_{sat}L_{sym}/K_{sat}$$

J. Margueron, R. Hoffmann Casali, F. Gulminelli, Phys. Rev. C 97, 025805 (2018)

C. Drischler et al., Phys. Rev. Lett. 125,202702 (2020)

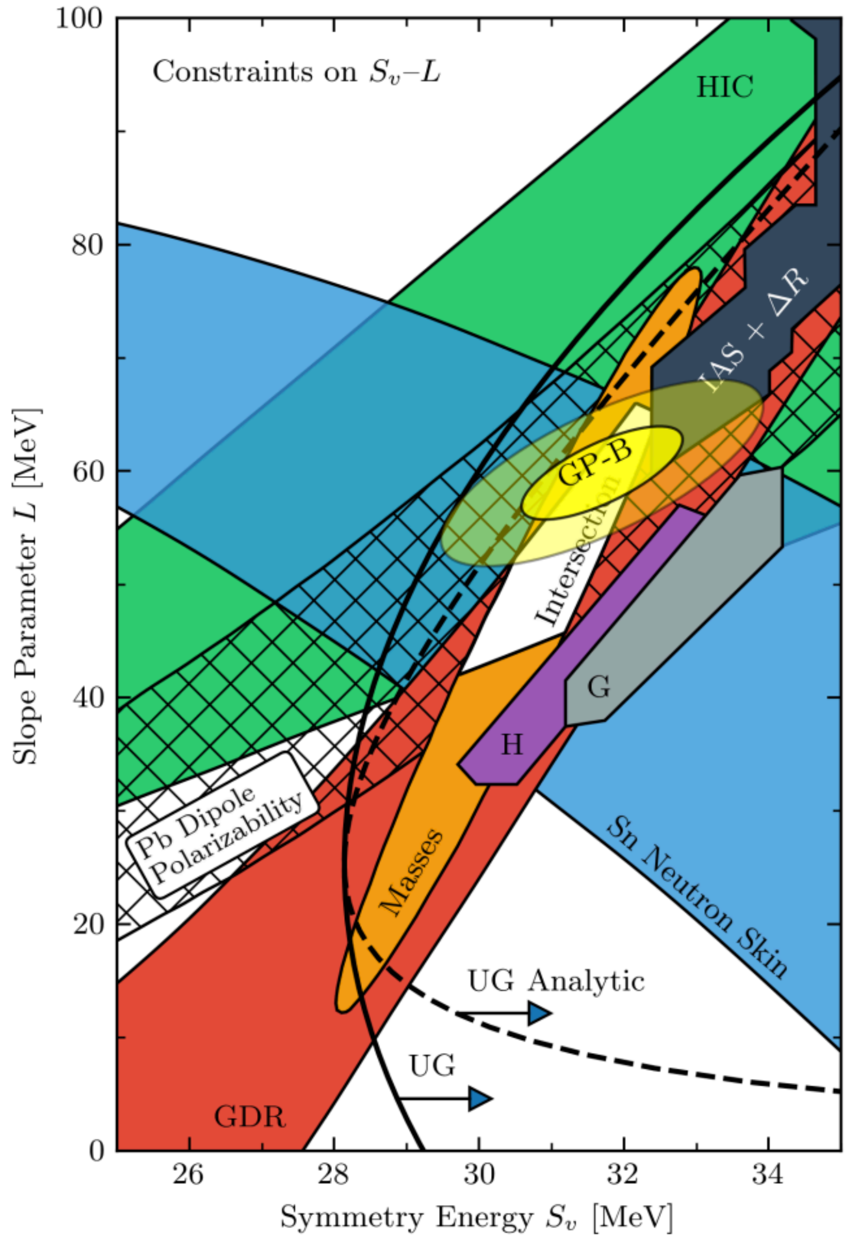

Results

Effect of the NICER constraint

We start our analysis by studying the effect of the astrophysical constraints, and in particular the effect of the NICER constraint

Effect of the NICER constraint

We start our analysis by studying the effect of the astrophysical constraints, and in particular the effect of the NICER constraint

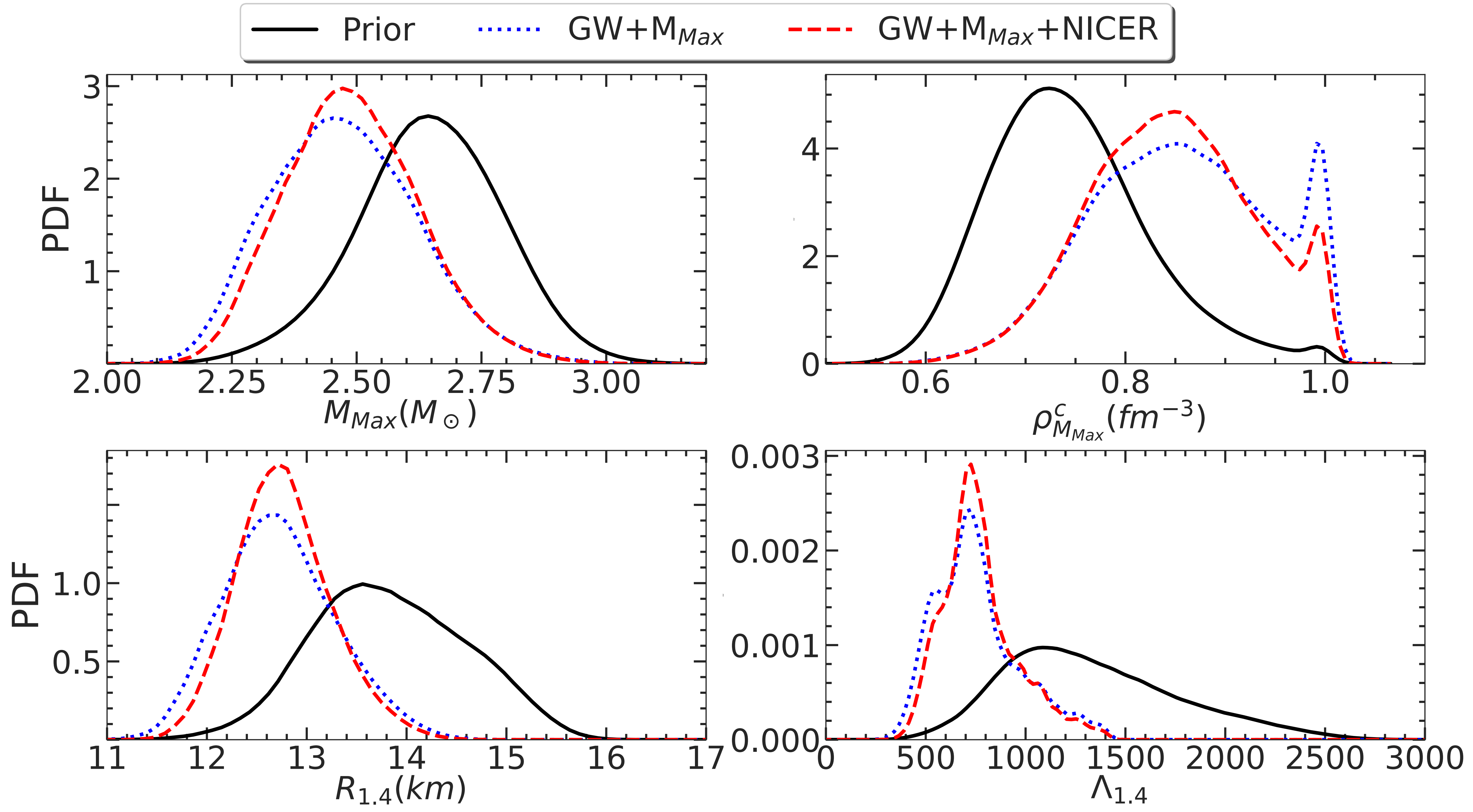

- **We see that the effect of the NICER constraint is subdominant with respect to the other astrophysical constraints. This is due to the big uncertainty in the NICER measurements of the radius**

Chiral-EFT Constraint

Our prior shows a very wide distribution for the proton fraction and the speed of sound at high densities

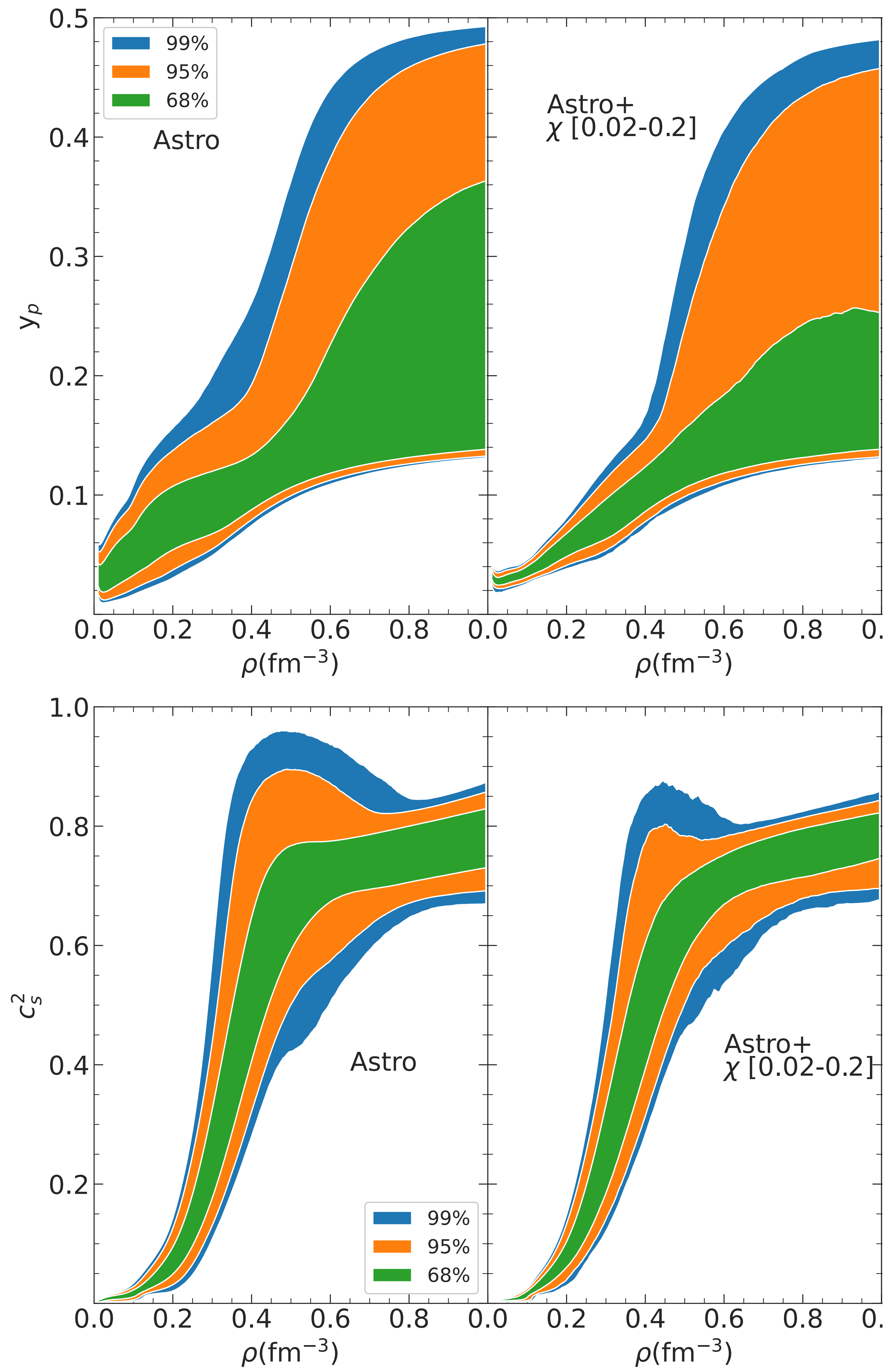

Chiral-EFT Constraint

Our prior shows a very wide distribution for the proton fraction and the speed of sound at high densities

On the other hand, nuclear constraints (and in particular the chiral-EFT constraint) strongly affect these quantities

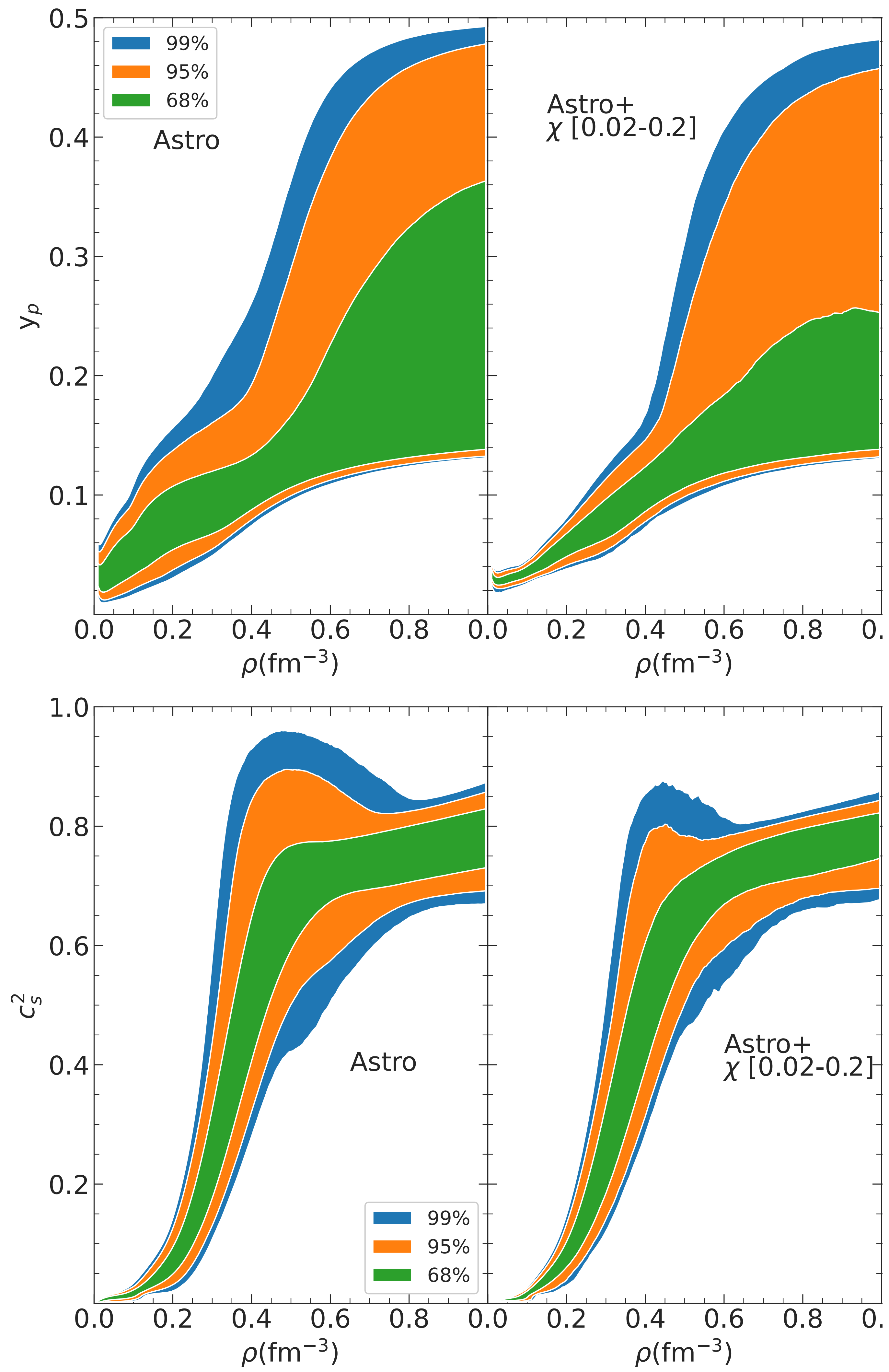

Chiral-EFT Constraint

Our prior shows a very wide distribution for the proton fraction and the speed of sound at high densities

On the other hand, nuclear constraints (and in particular the chiral-EFT constraint) strongly affect these quantities

The chiral-EFT constraint narrows the distribution of the proton fraction, favouring lower proton fractions. However, the posterior is still wider than in other RMF studies

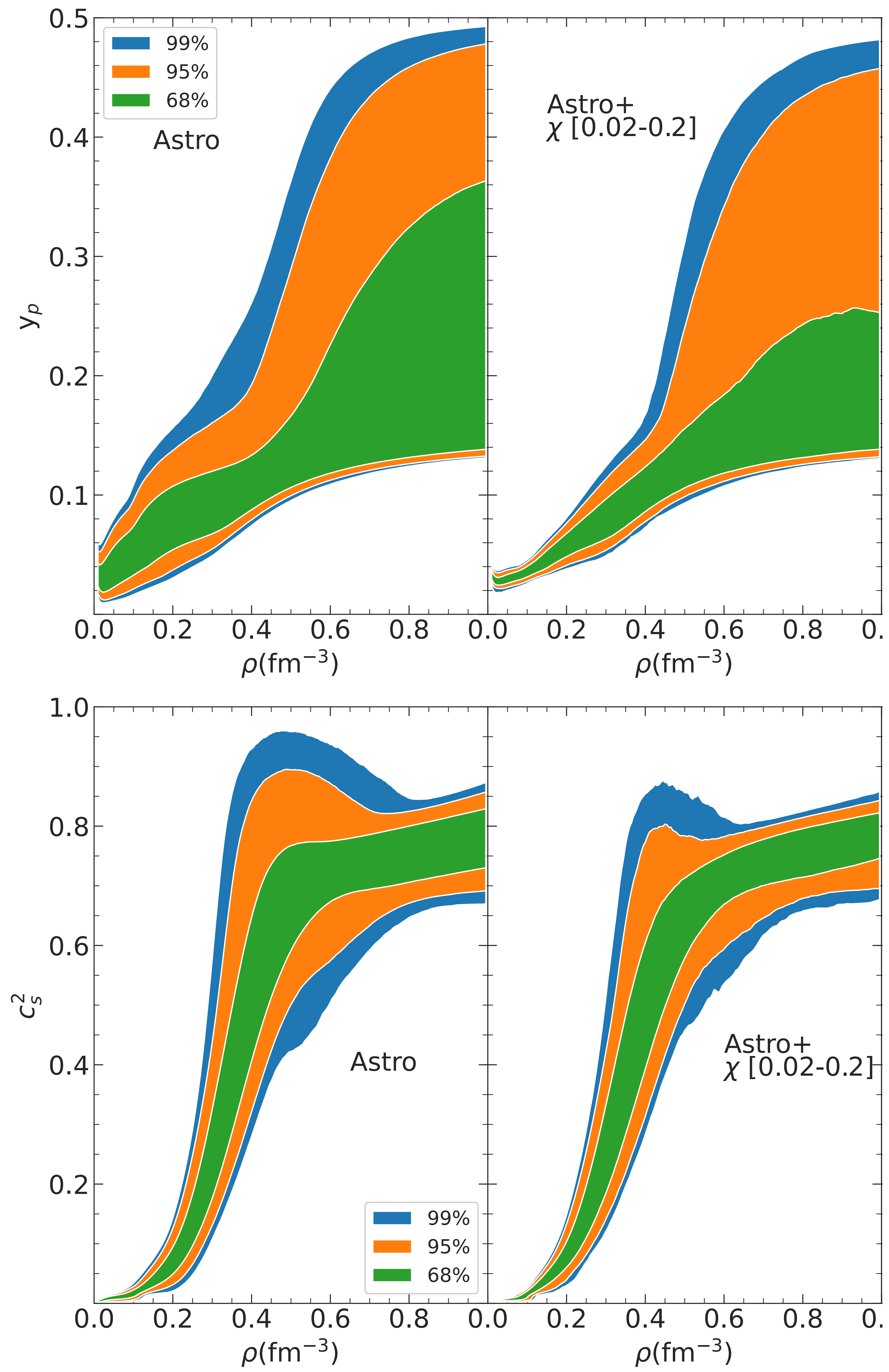

Direct URCA process

Direct URCA process

Direct URCA process is a very important cooling channel for NS

$$n \to p^+ + e^- + \bar{\nu}_e$$

$$p^+ + e^- \to n + \nu_e$$

Direct URCA process

Direct URCA process is a very important cooling channel for NS

$$n \to p^+ + e^- + \bar{\nu}_e$$

$$p^+ + e^- \to n + \nu_e$$

We can calculate if a model allows this process and at which density it becomes possible

$$y_p = \frac{1}{1 + \left(1 + x_e^{1/3}\right)^3}$$

$$x_e = \rho_e / (\rho_e + \rho_\mu)$$

Direct URCA process

Direct URCA process is a very important cooling channel for NS

$$n \rightarrow p^+ + e^- + \bar{\nu}_e$$

$$p^+ + e^- \rightarrow n + \nu_e$$

We can calculate if a model allows this process and at which density it becomes possible

$$y_p = \frac{1}{1 + \left(1 + x_e^{1/3}\right)^3}$$

$$x_e = \rho_e/(\rho_e + \rho_\mu)$$

In the final posterior we have roughly 70% probability of having direct URCA before $2.4 M_\odot$

We also see that the nuclear constraints rule out models with direct URCA at very low densities

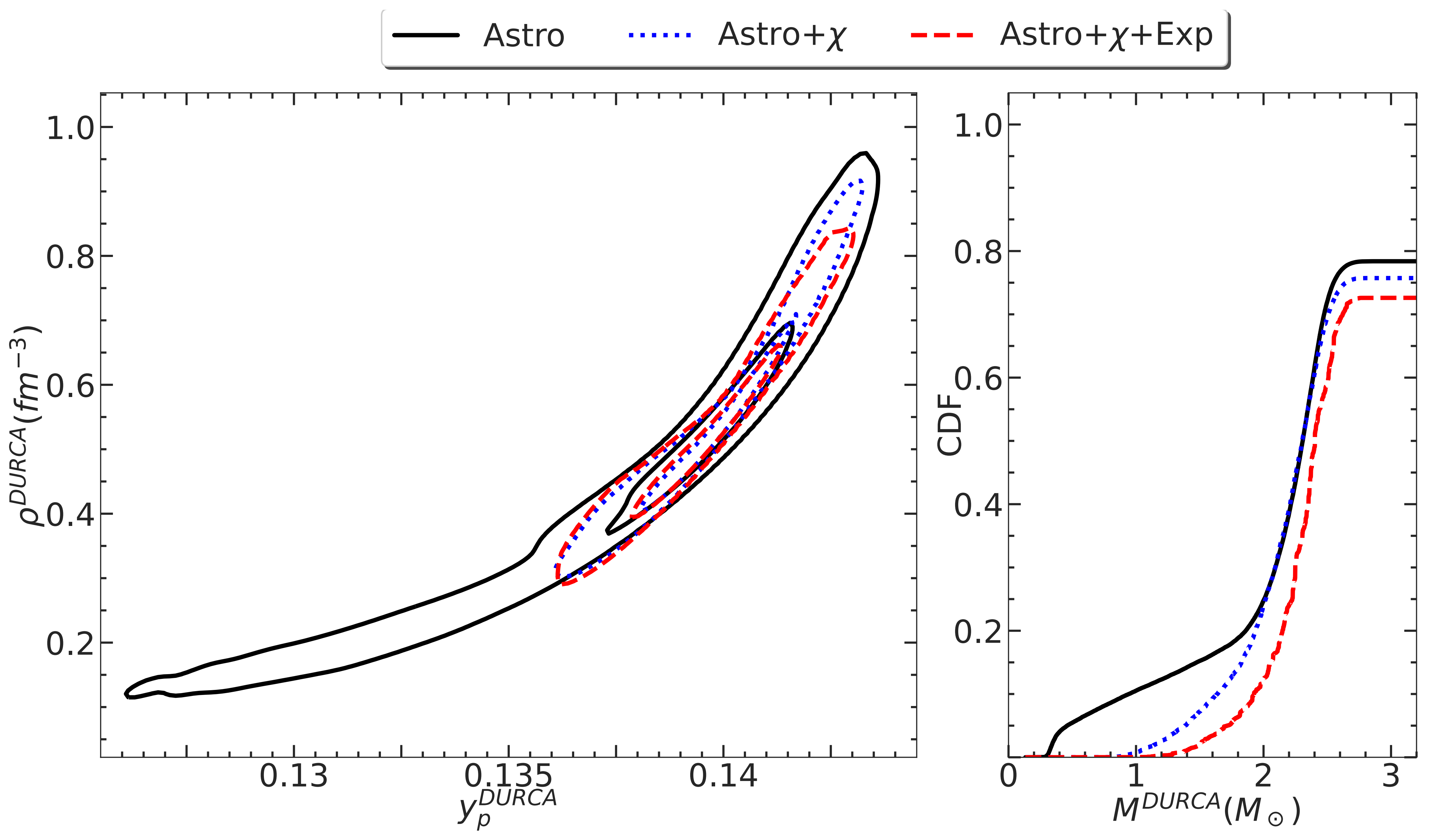

Conclusions

Conclusions

We perform a bayesin analysis to study the EoS of NS within a unified RMF framework. We study the effect of both nuclear and astrophysical constraints, in order to understand which properties of the internal structure were mostly affected.

- **We show that the constraint on the radius coming from the NICER measurements is weaker with respect to the one coming from the observation of GW170817**
- **We show that, in the unified framework, the chiral-EFT constraint tends to favour models with a lower proton fraction at high densities**
- **Finally, in our framework there is a high probability of observing direct URCA process in NS but a low probability of observing it for stars with** $M < 2M_\odot$

Publicly available models

We selected 5 of our models and uploaded them on the public database CompOSE

The models are selected to offer as much variety as possible in different physical quantities, while granting a good agreement with all the constraints

The whole dataset is now available on zenodo at

10.5281/zenodo.11084025

CompOSE
CompStar Online Supernovae Equations of State

https://compose.obspm.fr/eos/310

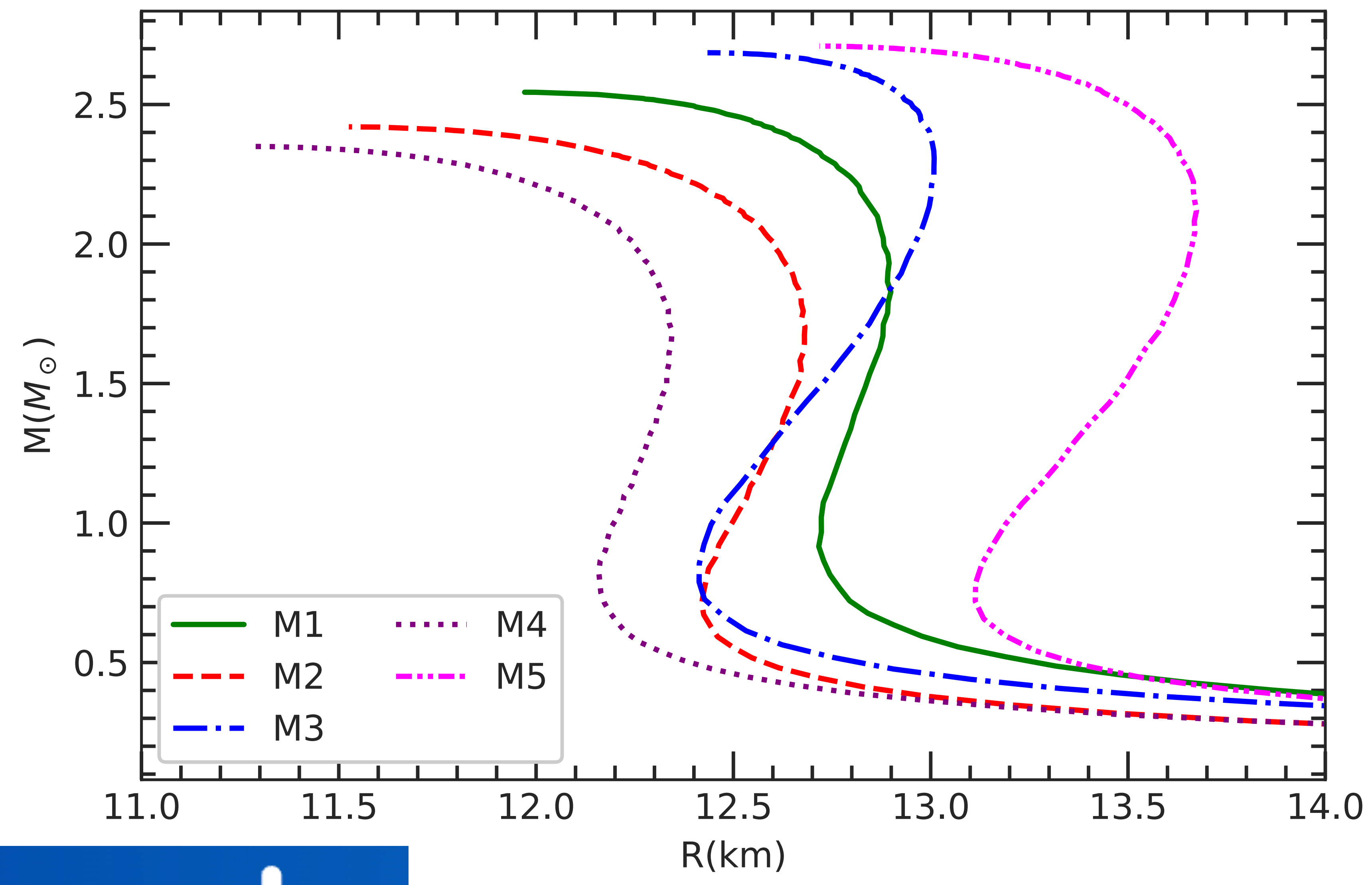

zenodo

PHYSICAL REVIEW D **109,** 103015 (2024)

General predictions of neutron star properties using unified relativistic mean-field equations of state

Luigi Scurto,[1,*] Helena Pais,[1,†] and Francesca Gulminelli[2,‡]
[1]*CFisUC, Department of Physics, University of Coimbra, 3004-516 Coimbra, Portugal*
[2]*Normandie Université, ENSICAEN, UNICAEN, CNRS/IN2P3, LPC Caen, F-14000 Caen, France*

(Received 23 February 2024; accepted 20 March 2024; published 10 May 2024)

In this work we present general predictions for the static observables of neutron stars (NSs) under the hypothesis of a purely nucleonic composition of the ultradense baryonic matter, using Bayesian inference on a very large parameter space conditioned by both astrophysical and nuclear physics constraints. The equations of state are obtained using a unified approach of the NS core and inner crust within a fully covariant treatment based on a relativistic mean-field Lagrangian density with density-dependent couplings. The posterior distributions are well compatible with the ones obtained by semiagnostic metamodeling techniques based on nonrelativistic functionals that span a similar portion of the parameter space in terms of nuclear matter parameters, and we confirm that the hypothesis of a purely nucleonic composition is compatible with all the present observations. We additionally show that present observations do not exclude the existence of very massive neutron stars with mass compatible with the lighter partner of the gravitational event GW190814 measured by the LIGO-Virgo Collaboration. Some selected representative models, that respect well all the constraints taken into account in this study and approximately cover the residual uncertainty in our posterior distributions, will be uploaded in the CompOSE database for use by the community.

DOI: 10.1103/PhysRevD.109.103015

Thank you !

Equilibrium conditions

The two phases must be in equilibrium with each other. The equilibrium conditions are obtained by minimising the energy density with respect to

- The fraction of liquid phase f
- The density of liquid phase ρ^I
- The proton density of liquid phase ρ_p^I

We obtain the following equilibrium conditions for the chemical potentials and pressure

- $$\mu_n^I = \mu_n^{II} - \mathscr{E}_{surf} \frac{3}{fB} \frac{\rho_p^I}{(\rho^I)^2} \left[\left(1 - \frac{\rho_p^I}{\rho^I}\right)^{-4} - \left(\frac{\rho_p^I}{\rho^I}\right)^{-4} \right]$$
- $$\mu_p^I = \mu_p^{II} - \frac{\mathscr{E}_{surf}}{(1-f)f(\rho_p^I - \rho_p^{II})} + \mathscr{E}_{surf} \frac{3}{fB} \frac{\rho_n^I}{(\rho^I)^2} \left[\left(1 - \frac{\rho_p^I}{\rho^I}\right)^{-4} - \left(\frac{\rho_p^I}{\rho^I}\right)^{-4} \right]$$
- $$P^I = P^{II} + \mathscr{E}_{surf} \left[\frac{3}{2\alpha} \frac{\partial \alpha}{\partial f} + \frac{1}{2\Phi} \frac{\partial \Phi}{\partial f} - \frac{((1-f)\rho_p^I + f\rho_p^{II})}{(1-f)f(\rho_p^I - \rho_p^{II})} \right]$$

$$B = \left[\left(\frac{\rho_p^I}{\rho^I}\right)^{-3} + b_s + \left(1 - \frac{\rho_p^I}{\rho^I}\right)^{-3} \right]$$

Bayesian framework

We construct a set of many differente EoSs and compare their predictions with the known experimental constraints

- Each EoS is identified as a set of N parameters $\mathbf{X}$ $\longrightarrow$ 12 coupling parameters
- Assign a probability to each model depending on how well it agrees with the constraints $\mathbf{c}$ $\longrightarrow$ $P(\mathbf{X}|\mathbf{c}) = \mathcal{N} \prod_k P(c_k|\mathbf{X})$
- Calculate the posterior marginalised distribution of the different quantities Y $\longrightarrow$ $P(Y|\mathbf{c}) = \prod_{k=1}^{N} \int_{X_k^{min}}^{X_k^{max}} dX_k \, P(\mathbf{X}|\mathbf{c}) \delta\left(Y - Y(\mathbf{X})\right)$

Effect of the NICER constraint

We start our analysis by studying the effect of the astrophysical constraints, and in particular the effect of the NICER constraint

- As expected, we see that the astrophysical observables are much more affected with respect to the crustal properties of the stars

- We see that the effect of the NICER constraint is subdominant with respect to the other astrophysical constraints. This is due to the big uncertainty in the NICER measurements of the radius

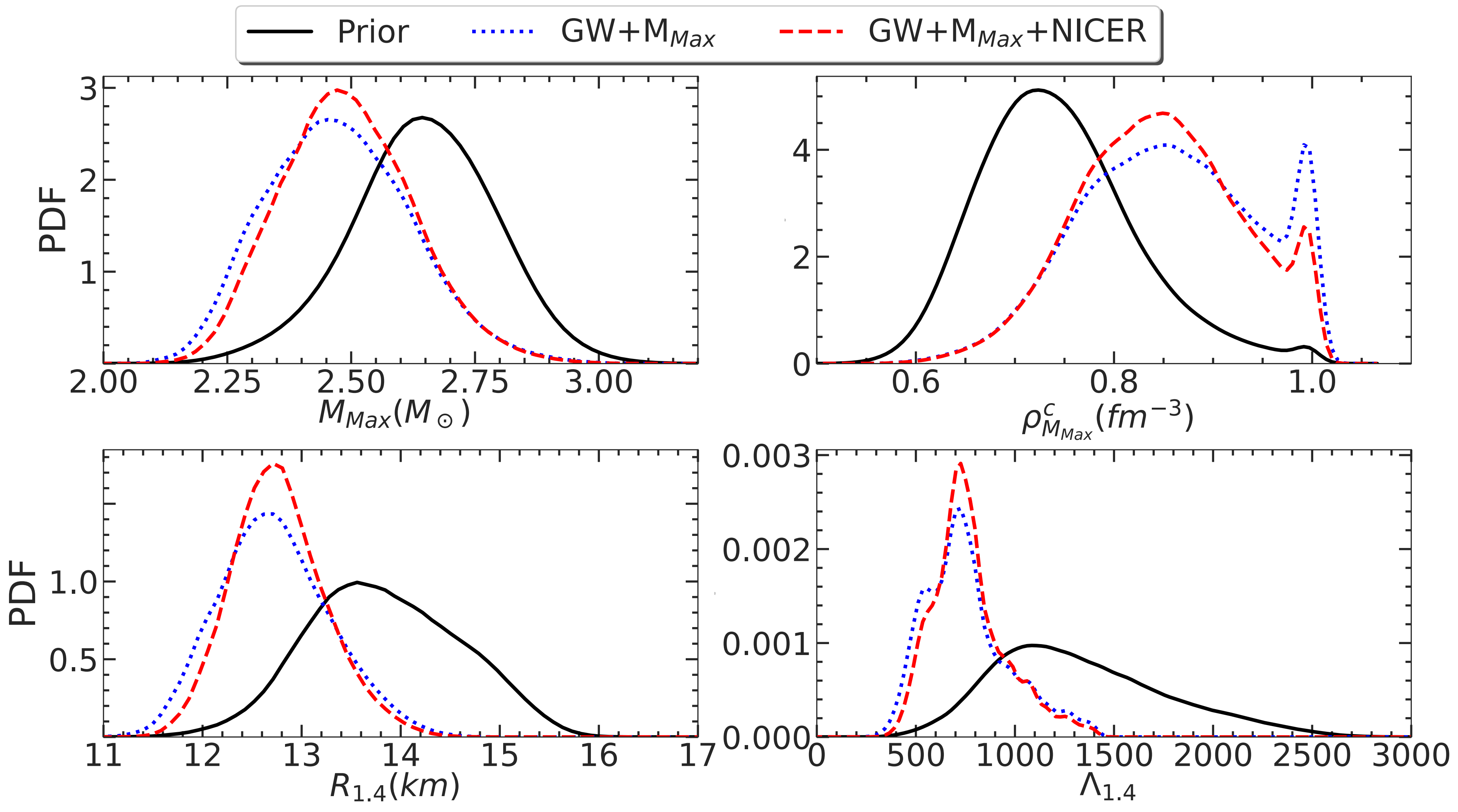

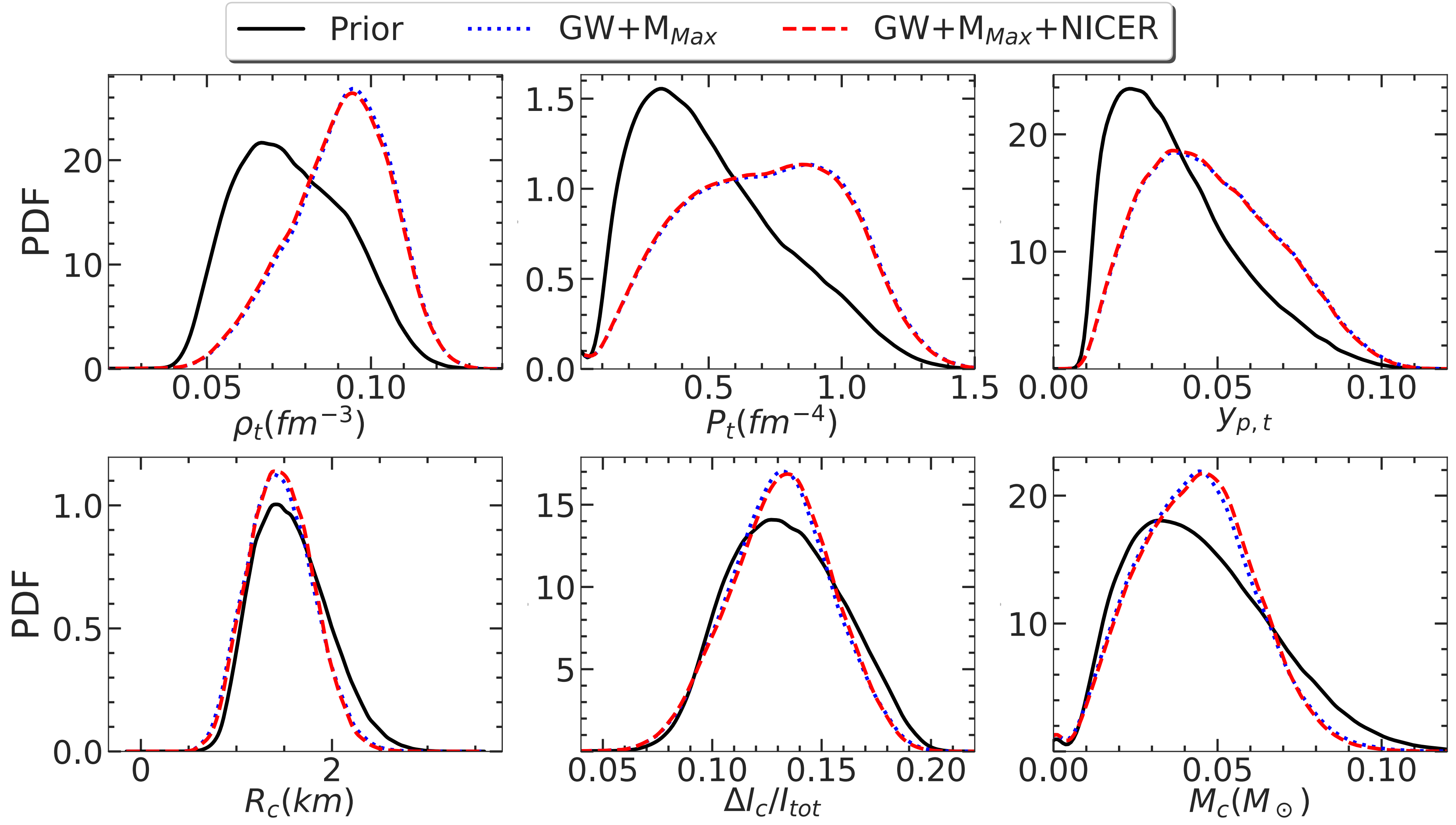

Chiral-EFT Constraint : implementation method

In our study, we implement the chiral-EFT constraint in two different ways

Heaviside Implementation

The probability distribution used to assign a probability to each model is

$$P(\chi\textbf{EFT}, HS \,|\, \mathbf{X}) \propto \prod_{i=1}^{N} \begin{cases} 1 & \textbf{if } x^i_{min} - \delta^i < x_i(\mathbf{X}) < x^i_{max} + \delta^i \\ 0 & \textbf{otherwise} \end{cases}$$

Where x^i_{min} and x^i_{max} are the extremes of the band given by the constraint

Gauss Implementation

The probability distribution used to assign a probability to each model is

$$P(\chi\textbf{EFT}, Gauss \,|\, \mathbf{X}) \propto \prod_{i=1}^{N} \begin{cases} P^i_U(x_i) & \textbf{if } x^i_{min} < x_i(\mathbf{X}) < x^i_{max} \\ P^i_G(x_i) & \textbf{otherwise} \end{cases}$$

Where

$$P^i_U(x) = \frac{0.682}{2\sigma_i} \qquad P^i_G(x) = \frac{1}{\sigma_i\sqrt{2\pi}} e^{-\frac{1}{2}\left(\frac{x' - \mu_i}{\sigma_i}\right)^2}$$

With $\mu_i = (x^i_{max} + x^i_{min})/2$ and $\sigma_i = (x^i_{max} - x^i_{min})/2$

Chiral-EFT Constraint : implementation method

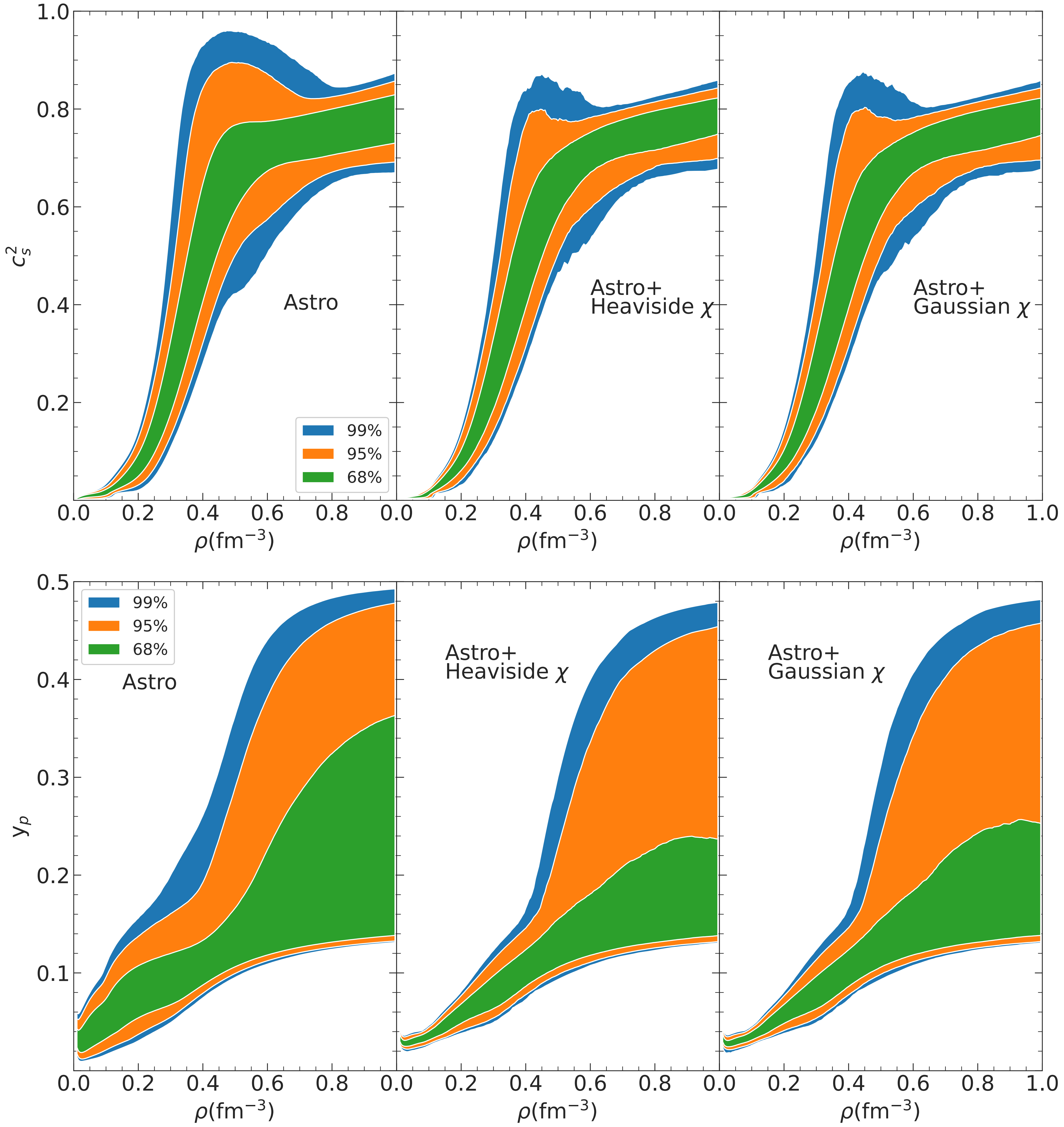

We compare the posterior distributions obtained with the two different implementations

Changing the way in which the constraint is implemented does not significantly affect the results

This allows us to have a higher number of models with a non-zero weight

Chiral-EFT Constraint : implementation range

We also compare the posterior distributions obtained by implementing the chiral-EFT constraint in two different density ranges

$[0.02fm^{-3} - 0.2fm^{-3}]$

$[0.1fm^{-3} - 0.2fm^{-3}]$

Our EoS are unified → Any constraint applied at low densities also have an effect at higher densities

PRO

More realistic description

No problems of jumps in quantities at the crust-core transition

CON

The way in which the low density constraints extend to high densities also depend on the specific model used for the EoS

Chiral-EFT Constraint : implementation range

For the proton fraction, we see a big difference at high densities already in the 68% quantile

↓

The big difference arises at densities higher than the central density of $2M_\odot$ stars

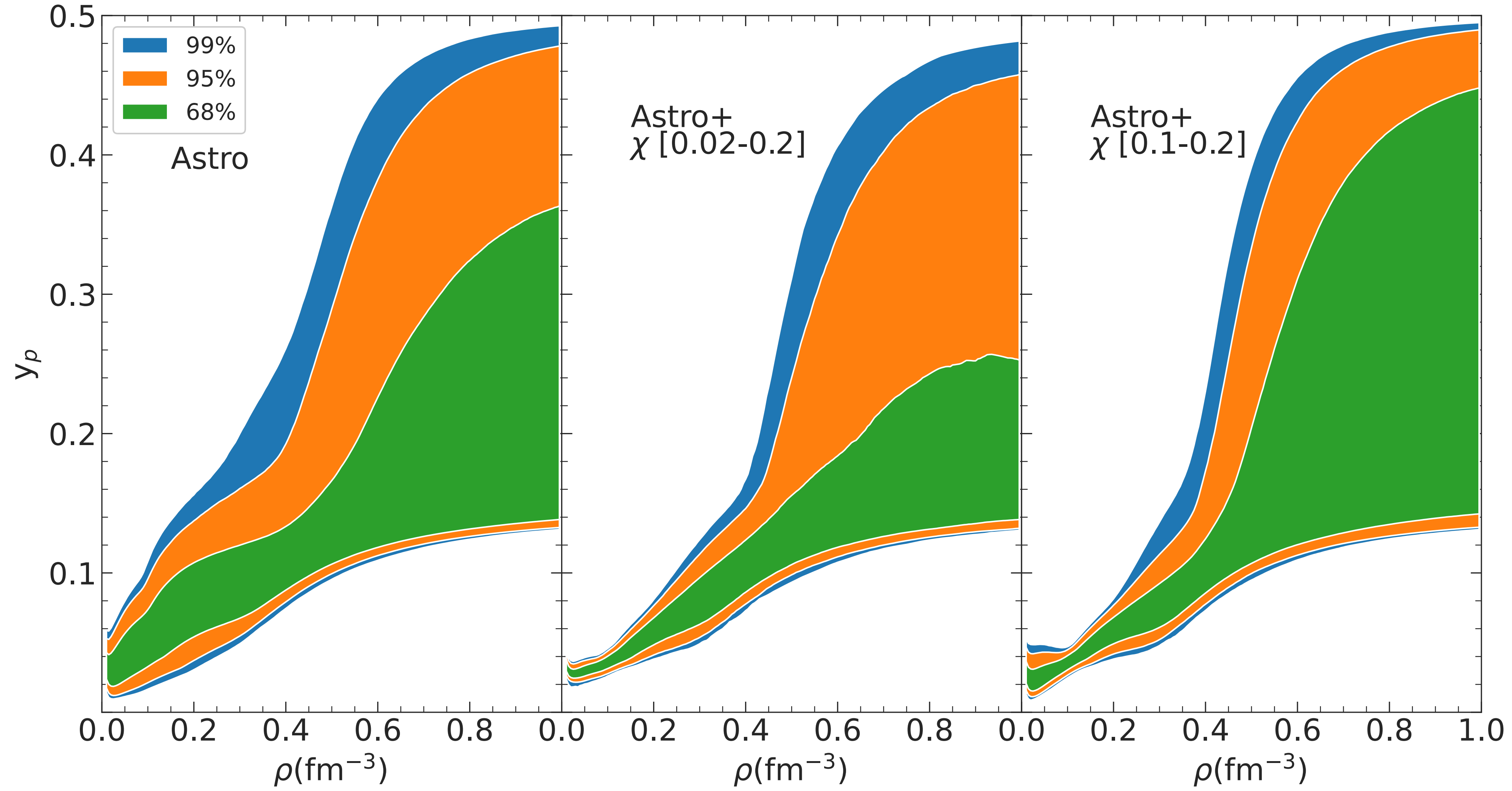

For the speed of sound, the main difference arises around $[0.4fm^{-3} - 0.7fm^{-3}]$

↓

The difference mainly involves the 95% and 99% quantiles

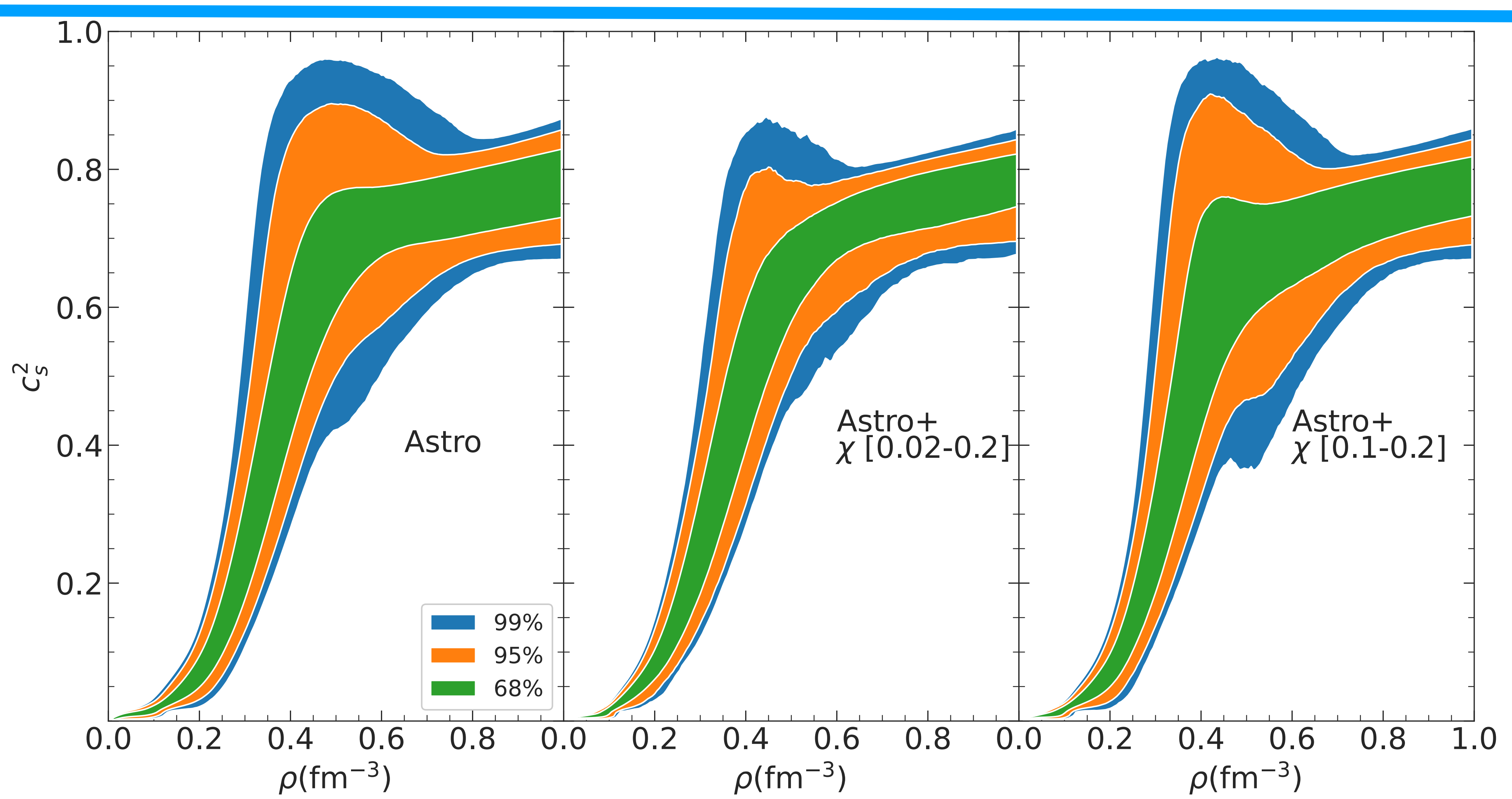

Chiral-EFT Constraint : connection to the couplings

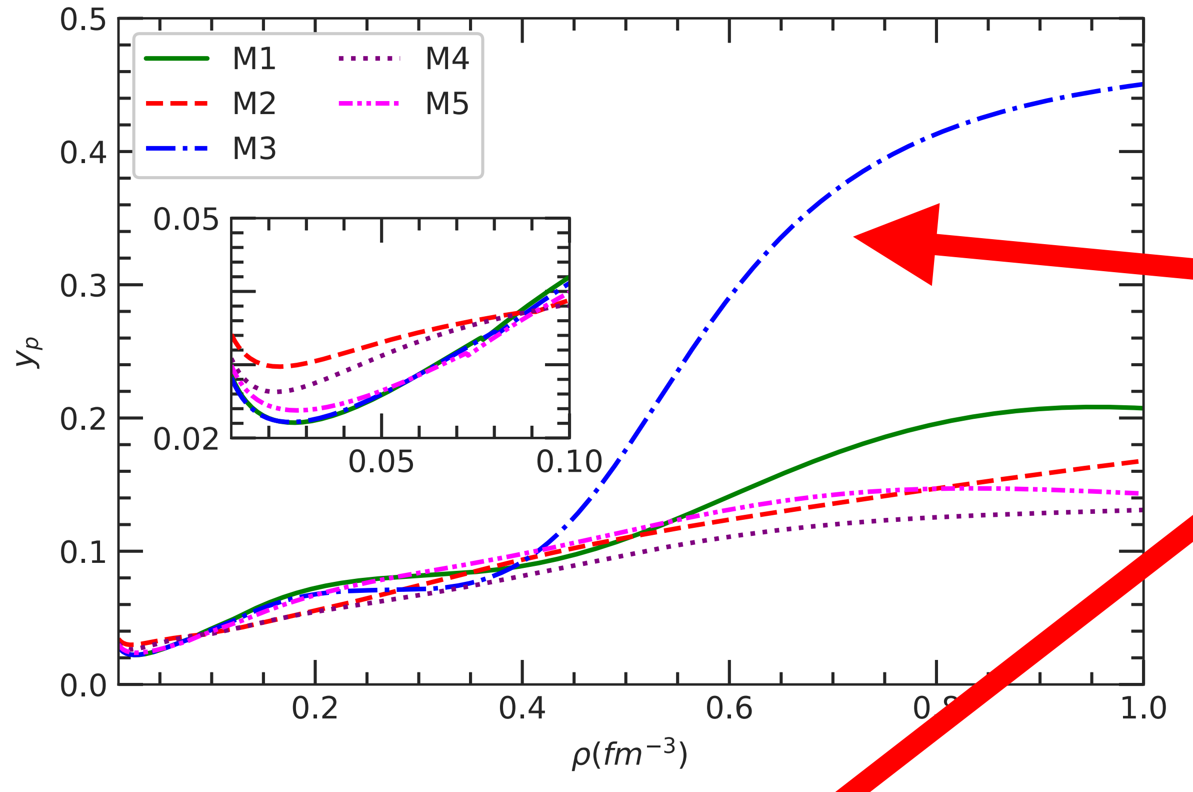

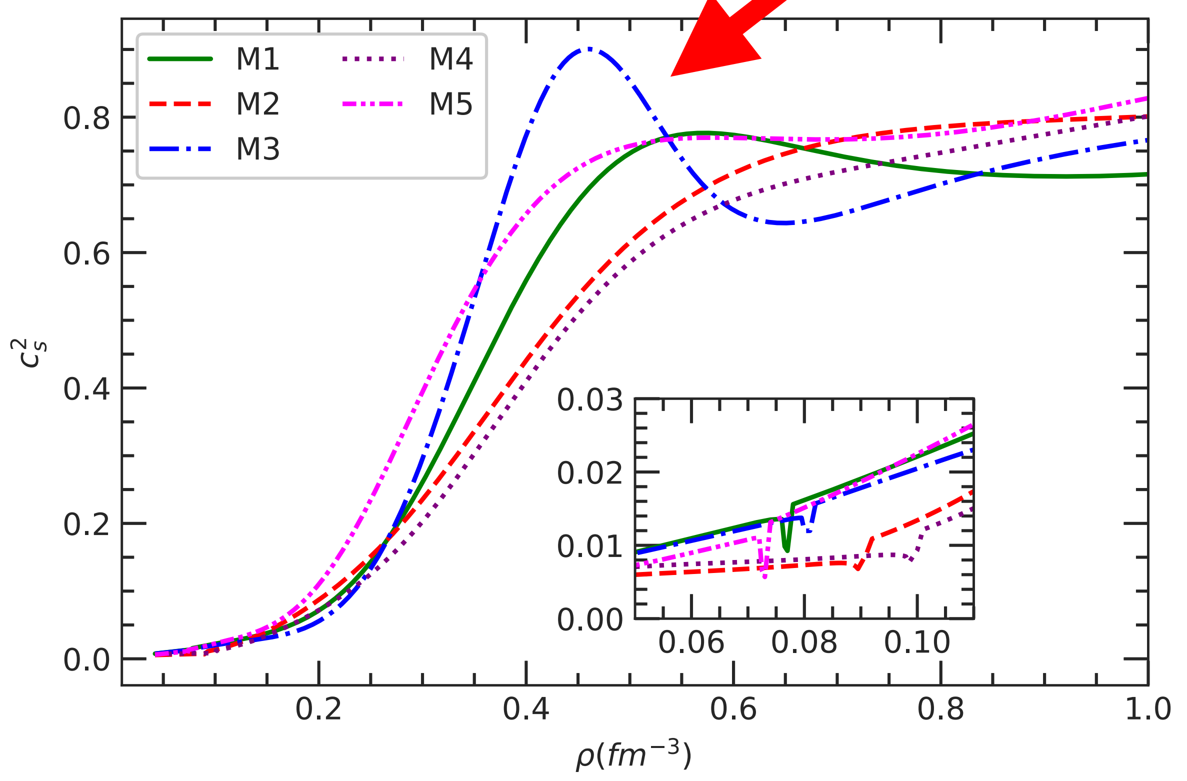

High proton fractions at high density and bumps in the speed of sound appear to be related to the behaviour of the isovector meson coupling

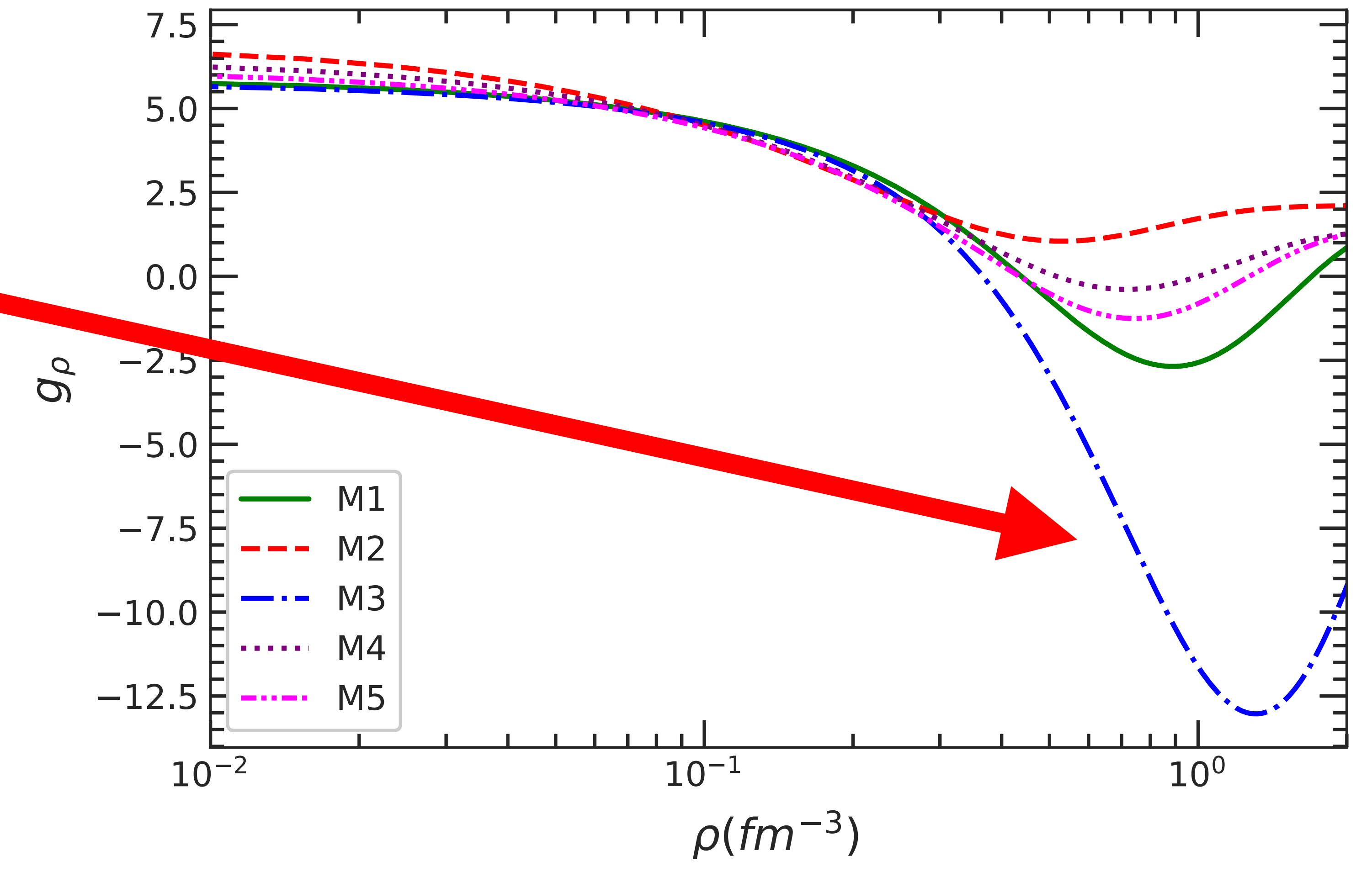

This shows the importance of having a flexible density functional for the couplings

It appears to also be related to backbending in the M-R plot

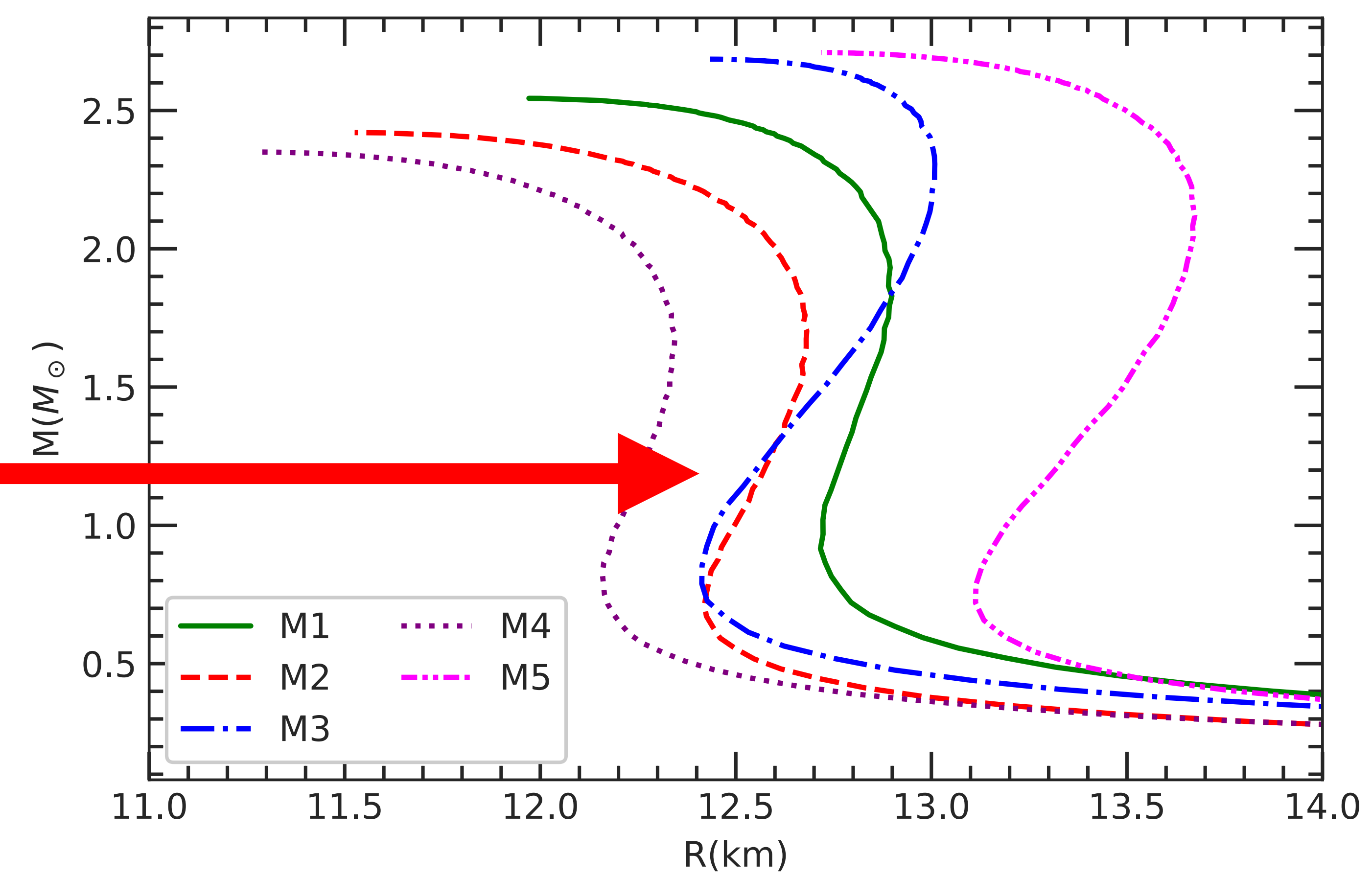

Experimental nuclear constraint

We proceed to study the effect of the experimental nuclear constraints in our posterior

The constraint appear to have a strong effect on the astrophysical observables, being more relevant than the chiral-EFT constraint

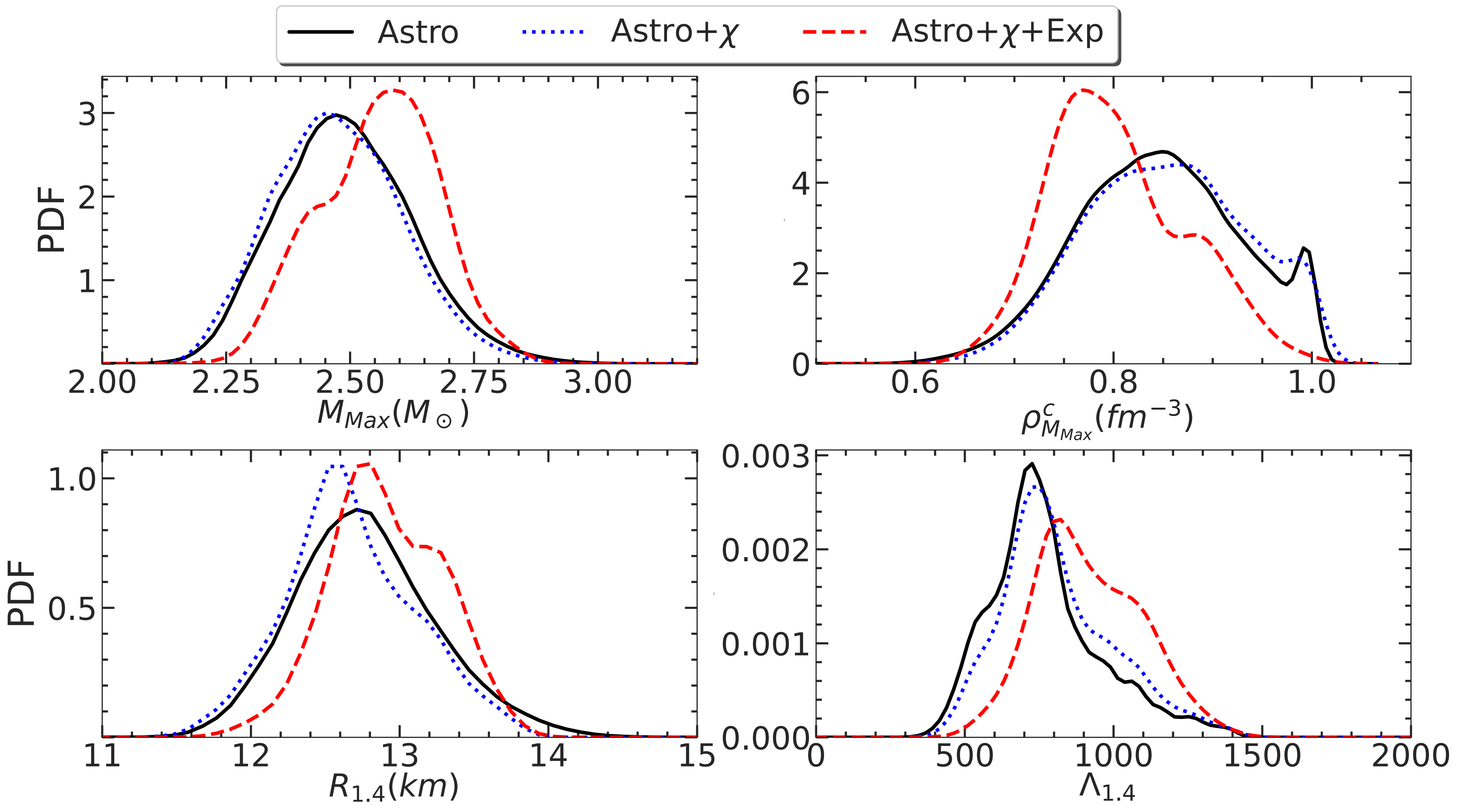

The opposite is true for the crustal properties, that are more effected by the chiral-EFT than the experimental constraint

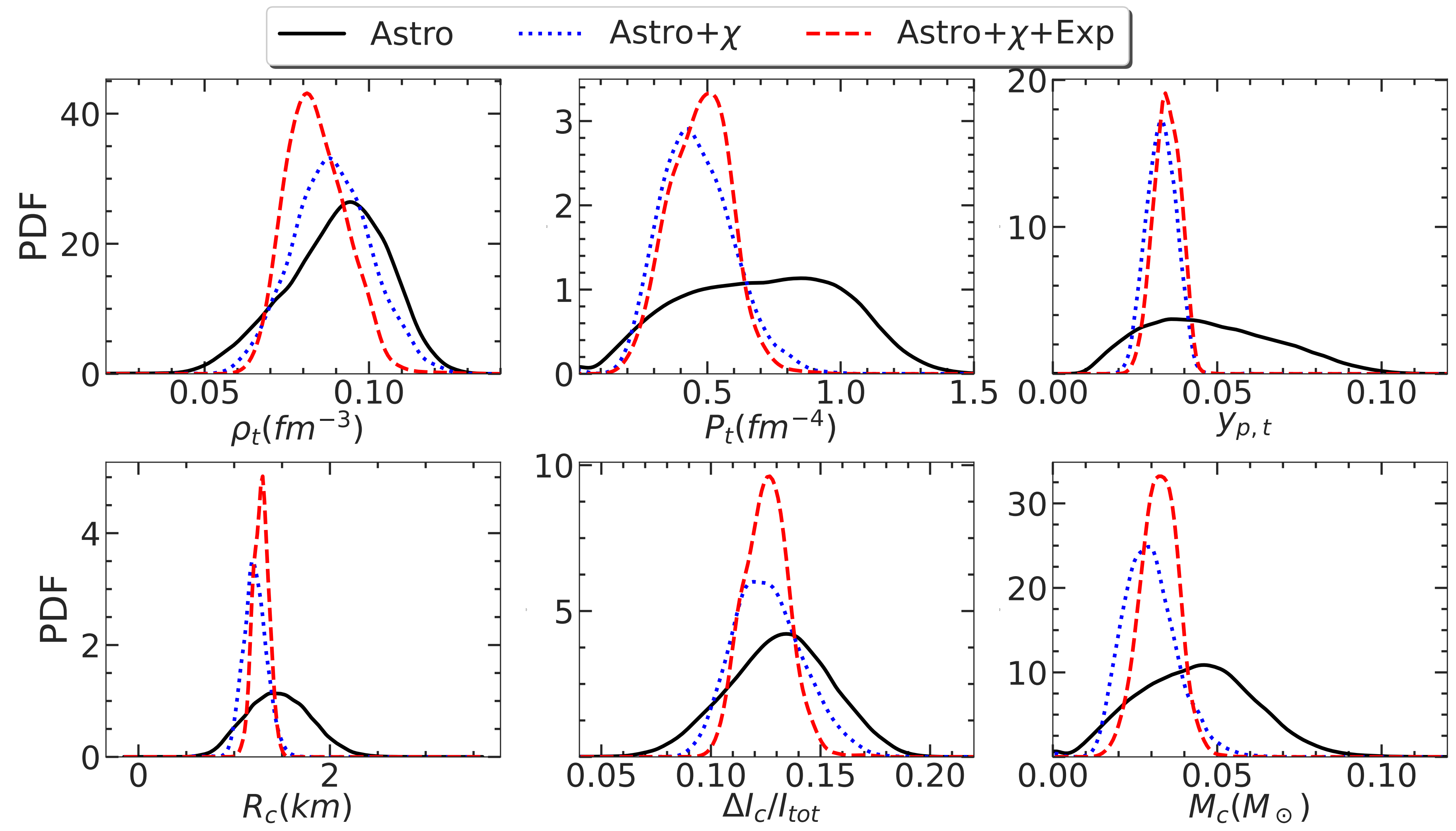

Experimental nuclear constraint

How can we explain this result ?

Astrophysical observables have strong correlation with two of the NMP that we directly constrain

Crustal properties have stronger correlation with the symmetry NMPs, that we do not directly constrain